

THESIS FOR THE DEGREE OF DOCTOR OF PHILOSOPHY
in
Machine and Vehicle Systems

Vehicle Dynamics Control after Impacts in Multiple-Event Accidents

DERONG YANG



Department of Applied Mechanics
CHALMERS UNIVERSITY OF TECHNOLOGY
Göteborg, Sweden 2013

Vehicle Dynamics Control after Impacts in Multiple-Event Accidents

DERONG YANG

ISBN 978-91-7385-887-8

Copyright © 2013 DERONG YANG. All rights reserved.

Doktorsavhandlingar vid Chalmers tekniska högskola

Ny serie nr 3568

ISSN 0346-718X

Department of Applied Mechanics

CHALMERS UNIVERSITY OF TECHNOLOGY

SE-412 96 Göteborg

Sweden

Phone: +46 (0)31 59 03 70

Email: derong.yang@chalmers.se

Typeset by the author using L^AT_EX.

Printed by Chalmers Reproservice
Göteborg, Sweden 2013

There is no problem, only solutions.

- John Lennon

Abstract

Accidents statistics show that multiple-event accidents (MEAs) represent a considerable and increasing proportion of all vehicle traffic accidents. MEAs are characterized by having at least one vehicle subjected to more than one harmful event. MEAs now comprise approximately 25% of all passenger vehicle accidents. This thesis aims to make systematic progress towards developing a vehicle Post Impact Control (PIC) function so as to avoid or mitigate any secondary event in MEAs.

To characterize the vehicle motion control problems for PIC, a number of MEAs from an accident database were analyzed. Post impact vehicle dynamics were studied considering the overall accident scenarios of exemplar cases. Reduction of kinetic energy and path lateral deviation were found to be most critical and beneficial for the vehicles after impacts.

To understand the mechanism of influencing the post impact vehicle path, numerical optimization was applied to minimize the maximum path lateral deviation. It was found that effective control can be achieved across a wide range of kinematic conditions, by switching between three sub-strategies established at vehicle body level. Results also showed that active front-axle steering, in addition to individual-wheel braking, provides significant control benefits, although not for all post-impact kinematics.

For closed-loop design of the path control, a Quasi-Linear Optimal Controller (QLOC) was proposed and verified with the numerical optimization results. The design method is novel – it well combines the linear co-states dynamics and nonlinear constraints due to tyre friction limits. The algorithm was further adapted to penalize both longitudinal and lateral path deviations, using a generalized cost function.

To verify the function with driver interaction, a number of exploratory methods were investigated regarding the driver safety, as well as the capability and accuracy to reproduce the real-world post-impact vehicle kinematics. A scheme of the function design for real-time implementation was proposed and applied to the experiments in a driving simulator environment.

Keywords: Vehicle Dynamics, Optimization, Path Control, Post Impact, Collision Avoidance, Multiple-Event Accidents, Accident Analysis.

Acknowledgements

This project was financed by Vehicle and Traffic Safety Centre at Chalmers (SAFER), Volvo Cars and Vinnova in Sweden. There are a number of people who have contributed to this project, herein, I would like to express my particular gratitude to some of them.

Prof. Bengt Jacobson has provided invaluable guidance throughout the project. I would not have started and finished this exciting doctoral study without Bengt's active role being "confusion sweeper". I always enjoy the enlightening discussions with my industrial supervisor Dr. Mats Jonasson, so that I remember I am working with cars, not only computers. Assoc. Prof. Mathias Lidberg and Prof. Anders Boström supervised me when Bengt was on parental leave, many thanks for the critical support. Assoc. Prof. Robert Thomson introduced and guided me in the early period of the project for which I am grateful. A lot of appreciation goes to Prof. Tim Gordon at University of Michigan, for the fruitful collaboration as well as making me believe that each discussion lasted only a minute.

I would like to thank Yujiao Song, Javier Beltran, Artem Kusachov, Faouzi Al Mouatamid, Pontus Petersson and Gonçalo Salazar for the contribution during their Master's thesis. Thanks go to Magdalena Lindman for the help in using the GIDAS database for accident analysis. Thanks go to Ulrich Sander for the references to the multiple-event accidents statistics. Thanks go to Karin Meinhardt Hallgren for the inputs on PIB function design. Thanks go to Bruno Augusto for the support in driving simulator tests. Thanks go to Johannes Edrén and Ivar Torstensson for the support to work with JModelica and Dymola/VDL models. Thanks go to Dr. Mattias Brännström and Dr. Mohammad Ali for the enjoyable discussions in vehicle control during my very first PhD course.

It is a privilege to do research in such an inspiring work environment, thanks to my colleagues at the Division of Vehicle Engineering & Autonomous Systems and the Division of Vehicle Safety at Chalmers. I will miss my student life here. Thanks go to Sonja Laakso Gustafsson and Marianne Hedfors for performing efficient administration. Dr. Matthijs Klomp and Dr. Sogol Kharrazi welcomed and impressed me with the excitement

ACKNOWLEDGEMENTS

to be a PhD student in the Vehicle Dynamics group, for which I am especially grateful. I also hope to extend my gratitude to Prof. Gunnar Olsson, Dr. Fredrik Bruzelius, Adithya Arikere, Anton Albinsson, Kristoffer Tagesson, Morteza Hassanzadeh Siyahpoush, Peter Nilsson and Ulrich Sander, for keeping such a dynamic group rhythm. Special thanks go to Andrew Dawkes for giving constructive advice on the language check.

Thanks to Prof. Tim Gordon, I had the opportunity to visit the Department of Mechanical Engineering at University of Michigan for three months. I enjoyed the wonderful time with the fellow students in the AutoLab. Thanks go to Mainak Mitra for showing me every coffee room of every department, and for inviting me to stimulating student parties. I would like to specially thank Anne Gordon for her warm hospitality during my stay in Ann Arbor.

I appreciate all the interesting discussions when sometimes working at the Division of Vehicle Dynamics Functions at Volvo Cars. I look very much forward to working with my colleagues there in future projects.

Deep gratitude goes to my dear friends and family for the never-ending support around. I am grateful to my parents for the unconditional care and positive characters that inspire me. I am so fortunate to have the incessant love and encouragement from my beloved husband Lei.

Derong Yang
Göteborg, August 2013

List of Publications

This thesis is based on the following appended papers:

Paper A

D. Yang, B. Jacobson, and M. Lidberg, “Benefit Prediction of Passenger Car Post Impact Stability Control Based on Accident Statistics and Vehicle Dynamics Simulations,” in *Proceedings of 21st International Symposium on Dynamics of Vehicles on Roads and Tracks*, Stockholm, Sweden, 2009.

The author of this thesis was responsible for accident data analysis, vehicle modeling, simulations and paper writing. The 2nd author assisted in vehicle modeling. The work was performed under the guidance of the co-authors.

Paper B

D. Yang, T. J. Gordon, B. Jacobson, M. Jonasson, and M. Lidberg, “Optimized Brake-based Control of Path Lateral Deviation for Mitigation of Secondary Collisions,” in *Proceedings of the Institution of Mechanical Engineers, Part D: Journal of Automobile Engineering*, vol. 225, no. 12, pp.1587–1604, 2011.

The author of this thesis was responsible for vehicle modeling, simulations and paper writing. The work was performed under the guidance of the co-authors.

Paper C

D. Yang, T. J. Gordon, B. Jacobson, and M. Jonasson, “Quasi-Linear Optimal Path Controller Applied to Post Impact Vehicle Dynamics,” *IEEE Transactions on Intelligent Transportation Systems*, vol. 13, no. 4, pp.1586–1598, 2012.

LIST OF PUBLICATIONS

The author of this thesis was responsible for vehicle modeling, mathematics derivation, simulations and paper writing. The 2nd author proposed the application of optimal control theory in the controller design. The work was performed under the guidance of the co-authors.

Paper D

D. Yang, T. J. Gordon, B. Jacobson, and M. Jonasson, “A Non-linear Post Impact Path Controller Based on Optimised Brake Sequences,” *Vehicle System Dynamics: International Journal of Vehicle Mechanics and Mobility*, vol. 50, no. suppl, pp. 131–149, 2012.

The author of this thesis was responsible for vehicle modeling, mathematics derivation, simulations and paper writing. The 2nd author was responsible for the writing of Appendix 1. The work was performed under the guidance of the co-authors.

Paper E

D. Yang, B. Jacobson, M. Jonasson, and T. J. Gordon, “Minimizing Vehicle Post Impact Path Lateral Deviation Using Optimized Braking and Steering Sequences,” *accepted for publication in International Journal of Automotive Technology*, accepted on March 19, 2013.

The author of this thesis was responsible for optimization problem formulation, simulations and paper writing. The work was performed under the guidance of the co-authors.

Paper F

D. Yang, M. Jonasson, B. Jacobson, and T. J. Gordon, “Closed-loop Controller for Post Impact Vehicle Dynamics Using Individual Wheel Braking and Front Axle Steering,” *submitted for publication in International Journal of Vehicle Autonomous Systems*, 2013.

The author of this thesis was responsible for controller design, vehicle model adaptation, simulations and paper writing. The work was performed under the guidance of the co-authors.

Paper G

D. Yang, T. J. Gordon, B. Jacobson, and M. Jonasson, “An Optimal Path Controller Minimizing Longitudinal and Lateral Deviations after Light Collisions,” *accepted for publication in Proceedings of 16th International IEEE Conference on Intelligent Transportation Systems*, Hague, The Netherlands, 2013.

The author of this thesis was responsible for vehicle modeling, mathematics derivation, simulations and paper writing. The 2nd author assisted in mathematics derivation. The work was performed under the guidance of the co-authors.

Paper H

F. A. Mouatamid, A. Kusachov, B. Jacobson, and D. Yang, “Towards Evaluation of Post Impact Braking Function in Driving Simulator,” *accepted for publication in Proceedings of the IEEE International Conference on Systems, Man, and Cybernetics*, Manchester, United Kingdom, 2013.

The author of this thesis was responsible for impact scenario selection and paper writing. The 1st and 2nd author were responsible for the PIB function implementation, experimental set-up, tests and data analysis. The work was performed under the guidance of the last two co-authors.

Other publications

In addition to the appended papers, the following publications by the thesis author are related to the topic of the thesis:

Paper I

D. Yang, “Method for Benefit Prediction of Passenger Car Post Impact Stability Control,” Master’s Thesis 2009:06, ISSN 1652-8557, Gothenburg, Sweden, Chalmers University of Technology, 2009.

Paper J

D. Yang, T. J. Gordon, M. Lidberg, M. Jonasson, and B. Jacobson, “Post-Impact Vehicle Path Control by Optimization of Individual Wheel Braking Sequences,” in *Proceedings of 10th*

LIST OF PUBLICATIONS

International Symposium on Advanced Vehicle Control, Loughborough, United Kingdom, 2010, pp. 882–887.

Paper K

B. Jacobson, D. Yang, M. Thor, J. Lu, and M. Lidberg, “Potential Effectiveness of A Stability Control System for Passenger Cars after An Initial Side Impact,” *submitted for publication in Proceedings of FISITA 2014 World Automotive Congress*, Maastricht, The Netherlands, 2013.

Patent

D. Yang, M. Jonasson, B. Jacobson, and T. J. Gordon, “Special method for road friction estimation,” *to be submitted for patent application*, No. I3109SE00, 2013.

Contents

Abstract	i
Acknowledgements	iii
List of Publications	v
Contents	ix

I Introductory Chapters

1 Overview	1
1.1 Research motivation	1
1.2 Research question	1
1.3 Research scope	3
1.4 Research limitations	5
1.5 Scientific contribution of this thesis	7
1.6 Thesis outline	9
2 Literature Review	11
2.1 Statistics of multiple-event accidents	11
2.2 PIC-relevant functions	12
2.3 Methods for ESC benefit evaluation	14
3 Vehicle Dynamics after Impacts	17
3.1 Driver reactions after impacts	17
3.2 Accident reconstruction	18
3.3 PIC-relevant cars in real-world accidents	19
3.4 Phase portrait and bifurcation characteristics	22
3.5 Case-by-case analysis	24
3.5.1 Causes of secondary events	25
3.5.2 Benefits evaluation using example controller	25

CONTENTS

4	Optimal Control Synthesis	27
4.1	Optimization methods	28
4.2	Minimization of path lateral deviation	29
4.3	Optimal vehicle-level control strategies	32
4.3.1	Phase plane analysis	32
4.3.2	Lateral force control	35
4.3.3	Yaw moment control	36
4.4	Generalization of cost functions	37
4.4.1	Cost functions for crash risks	38
4.4.2	Cost functions for crash severity	39
5	Optimal Post Impact Path Controller Design	41
5.1	Optimal path control methods	41
5.2	Quasi-linear optimal controller	43
5.2.1	From optimal control theory to path control problem	43
5.2.2	Candidate solutions to the BVP	47
5.2.3	Closed-loop controller	48
5.3	Under-determination in control allocation at tyre friction limits	50
6	Function Design and Verification in Experiments	55
6.1	Function design	55
6.2	Verification methods for driver interaction	58
6.2.1	Precision immobilization technique	58
6.2.2	Destabilization using built-in actuators	60
6.2.3	Kick plate	62
6.2.4	Motion-based driving simulator	63
6.2.5	Summary of verification methods	65
6.3	Verification in driving simulator	66
7	Conclusions and Recommendations for Future Work	69
7.1	Conclusions	69
7.2	Recommendations for future work	70
	References	73
	Nomenclature and Glossary	83

II Included Publications

Part I

Introductory Chapters

Chapter 1

Overview

1.1 Research motivation

Vehicle traffic safety has been attracting considerable attention from all perspectives, given the continuing high numbers of accidents registered in road traffic statistics. One type of accident is gradually increasing according to the recent accident statistics: multiple-event accidents (MEAs) [1]. These are characterized by having at least one vehicle subjected to more than one harmful event, such as collision with another vehicle or object. Statistics show that MEAs comprise approximately 25% of all passenger vehicle accidents [2–4]; in particular, two-impact accidents account for about 70% of all planar MEAs which have no roll-over [3, 5, 6]; and human injury levels in MEAs are higher than in single-event accidents (SEAs), with more than one third of accidents with severe (i.e. AIS3+) injuries being MEAs [3, 4, 7]. Studies on more recent accident statistics show that MEAs have a three-fold risk for severe and four-fold risk for fatal injury compared to SEAs; on average, 50% of all passenger vehicles suffering MEAs have the severe injuries sustained in one or several subsequent impacts [6].

The research motivation is hereby the following real-world problem: *Vehicles and human beings are subjected to more than one hazardous event in the traffic accidents.*

1.2 Research question

The concerns arising around vehicle and traffic safety, actively incorporate relevant research in academia while also propelling safety systems development in the automotive industry. Nowadays, vehicle safety systems are widely categorized as *preventive* systems which aim to prevent the imminent crashes; and *protective* systems which protect the human beings by

reducing injuries.

In the recent decades, various vehicle dynamics control functions have been widely industrialized as active safety systems on-board that have substantially contributed to the reduction of injuries and damage in traffic accidents. The most relevant one connected to the MEAs problem described above is the Electronic Stability Control (ESC) system; this functionality is being continuously improved by several added-valued features, e.g. rear-axle side-slip control, roll-over mitigation, trailer sway control [8] etc. Although there exist numerous names and versions of ESC algorithms on the market, the fundamental principle is mostly the same: deduce and follow the driver's intended yaw rate within the limits of various stability criteria [9–13], by active braking and steering which re-distributes the tyre longitudinal and lateral forces, so as to improve vehicle handling performance near the limit of tyre-road adhesion.

On-track tests and accident statistics show that ESC can effectively stabilize the vehicle yaw instability due to external disturbances of low amplitudes, e.g. aggressive driver manoeuvres, side-winds and uneven tyre friction. A general figure of ESC effectiveness summarized from the accident studies by Linder et al. is around 20-50%, which largely depends on vehicle type, injury severity level, type of accident, road conditions etc [14]. Considering the most ESC-pertinent types of accidents, it was estimated that about 35% less risk is expected for cars getting into serious accidents when equipped with ESC, compared with the ones without ESC [15]. A literature review by Ferguson came to the conclusion that in the USA, fatal single-vehicle crashes involving cars are reduced by about 30-50% and SUV by 50-70%. Fatal rollover crashes are estimated to be about 70-90% lower with ESC regardless of vehicle type. There is little or no effect of ESC in all multi-vehicle crashes [16]. Generally, ESC effectiveness is seen as improved when the road condition is slippery [16].

However, there is no evidence indicating that current ESC systems can handle relatively high amplitudes of disturbances, such as an impact, onto the car body. Firstly, during the impact, the sensors signals could be implausible due to high accelerations and velocities, in which case ESC could be deactivated. Secondly, after the impact, the vehicle is exposed to violent spinning and skidding motions which are likely to be beyond the efficient operation range designed by current ESC algorithms. In most cases, even if the stabilization can eventually be achieved, it takes too much time and space so that the probability of a secondary event is hardly lowered [17]. Thirdly, the main reference of ESC interventions is derived from the driver, who is possibly unable to act correctly to accomplish a successful avoidance

manoeuvre during and after the impact¹.

The research question that appears is: *How to control the post impact vehicle motion in order to avoid or mitigate the secondary events in multiple-event accidents?*

1.3 Research scope

The present research aims to provide a new active safety function that controls the post impact vehicle motions for avoiding or mitigating the secondary events in MEAs, named Post Impact Control (PIC) below. Here *secondary* can be a general term that defines the event directly *following* a primary impact in MEAs. The function is envisioned to be triggered by traditional sensors for passive safety systems such as airbags. The traditional chassis actuators, i.e. individual wheel brakes and active front axle steering are considered. The environment sensors on the current generation of active safety systems, e.g. radar and camera used by Autonomous Emergency Braking (AEB) are also considered as suitable, although not strictly necessary for a PIC function. Figure 1.1 illustrates a PIC-relevant car in a typical MEA scenario at an intersection; the host car is struck laterally by a bullet car whereafter its dynamics become disturbed and it runs into the guardrail on the roadside. The vehicle post-impact states are also highlighted in the figure. Here PIC-relevant is defined as: positive safety benefit is foreseen with the interventions of post impact vehicle control.

The well-known Haddon’s Matrix gives the human injury reduction in the presence of the potential hazards over one entire accident [18]. It interprets the different roles of various vehicle safety systems, driver and environment, in order to prevent or attenuate the harm occurring at each phase of the accident. Here the matrix is populated with the up-to-date systems and slightly extended for PIC function, see Figure 1.2. It implies that after the initial impact, apart from protecting occupants by deploying passive safety systems, active vehicle control such as PIC systems could also be triggered. The inevitability level for the subsequent collision increases from left to right as the accident evolves.

One initial thought about post impact control is to simultaneously apply ABS-braking or partial braking on all four wheels, generally named Post Impact Braking (PIB). This type of secondary collision brake assist systems is now emerging on the market [19–21]. PIB autonomously reduces the vehicle longitudinal speed significantly with relatively low requirement

¹In this thesis, these three words are the same and thus inter-changeable: impact, collision, crash, which are adopted according the terminology of different topics in the traffic safety research fields.

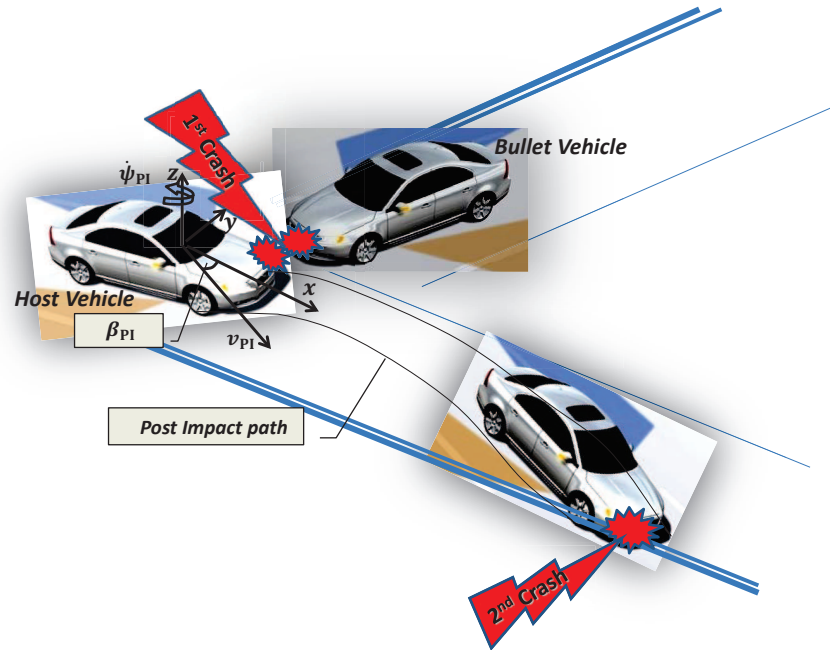


Figure 1.1: PIC-relevant car involved in a MEA. (v_{PI} : post-impact velocity, $\dot{\psi}_{PI}$: post-impact yaw rate, β_{PI} : post-impact side slip angle.)

on the sensors; on the other hand, other potential hazards remain, e.g. collision from behind and deviation from the original lane. In general it is a complex problem to determine the exact hazard function which can well describe the crash risk and severity to be minimized by PIC function. This largely depends on the information of road geometry and traffic situation that should be continuously updated using certain environment sensing and telematics systems. Whereas the on-line estimation of such hazard function is left outside the scope of this thesis, PIC aims to minimize the crash risk based on the *prescribed* cost functions of the foreseen collision risks. In this context, one variant of PIC function in particular is to tackle vehicle directional control problems after the initial impact; it can be referred to as Post Impact Stability Control (PISC). Here *Stability* is used in a general way; it does not only mean to stabilize the velocities, but also to achieve preferable displacements and orientations which would eventually influence the probabilities of secondary events.

Statistics about vehicle dynamic states after impacts are not found in any published study of accident databases; therefore in-depth, even if not exhaustive, accident analysis can be an invaluable first step, so as to identify the cars with potential to gain safety benefits from PIC. Based on the real-

HADDON's Matrix extended for MEAs	Pre-accident			Accident			Post-accident
	Normal Driving	Collision Avoidance	Collision Imminent	1st Collision	Post 1st Collision	Secondary Events	
Vehicle	ADAS: Night vision, Alco-lock, BLIS, TPMS, ABL, DAC, ACC etc.	ADAS: LDW, DAC, FCW etc.	Active Vehicle Dynamics Control: Active Steering, AEB etc.	Robust crash detection, verification and characterization	Active Vehicle Dynamics Control: PIB, PISC	Passive Safety: Seatbelt, Airbag, IC, WHIPS, Collapsible steering column, Pedestrian Protection etc.	Event data recorder, minimized likelihood of post-impact fire on oil tank, etc.
		Active Vehicle Dynamics Control: ABS, ESC, RSC, ASR, RWS etc.	Passive Safety: Seatbelt pretension, Energy-absorbing structures etc.	Passive Safety: Seatbelt, Airbag, IC, WHIPS, Collapsible steering column, Pedestrian Protection etc.			Automatic call for ambulance etc.
Driver	Qualified driving education	Proper interaction with vehicle	Not panic, correct manoeuvre	High physical tolerances to crash forces, wearing seatbelt etc.	Alert, no panic, skilled manoeuvre	Alert, no panic, skilled manoeuvre	Survived or minimally injured
Environment	Clear road signs, paving conditions, GPS etc.	Rumble stripes, sensors on infrastructure etc.	Rumble stripes	Guard rails and other fixed object near roadway	Qualified sensors on infrastructures, road maps	Qualified sensors on infrastructures, road maps	Effective emergency response, social system for victim rehabilitation

Figure 1.2: Extended Haddon's matrix, describing different roles in *multiple-event accidents*.

world crash scenarios found in accidents studies, the method to predict the benefit and risk of PIC can be constructed. Vehicle dynamics control algorithms can thus be designed according to the real-world requirements attributed to the mitigation of secondary events. Verification of the PIC function appears to be a challenge concerning both the driver interaction and vehicle actuators.

1.4 Research limitations

The subjects which are closely related to the PIC function development but not covered in the present research work are:

- Algorithms for impact detection, verification and characterization. That is to say, the threat assessment and decision-making issues are not studied. However, the PIC function in this thesis decides the impact detectability based on the capabilities of state-of-art crash and vehicle dynamics sensor technologies, and provides the specification of certain quantities which need to be characterized for properly triggering the controller.

- Algorithms for signal processing, e.g. state and parameter measurement and estimation. To achieve the optimal solution using the PIC function proposed in this thesis, certain parameters (road friction, road geometry, obstacle characteristics etc.) and vehicle dynamics states (yaw rate, yaw angle, side slip angle etc.) should either be measured or estimated in real time.
- Complete statistical study on the safety benefit and risk of PIC function, in terms of financial cost to the whole of society. This especially requires a comprehensive probabilistic approach to define the traffic environment, e.g. weather, time of the day, oncoming/following traffic, position and property of other obstacles etc. These confounding factors will affect not only the PIC-relevant cars but also the third parties involved.
- One large population, the cars involved in single-event accidents are not studied in this thesis. This population would determine some possible risks, such as hit by a car from behind, caused by the PIC intervention assuming the *exact* scene which existed in the real accident. On the other hand, the single-event cars might have been exposed to multiple-event accidents given *other* traffic environment and road conditions etc, and hence would gain potential benefits if PIC was activated on the scene.
- The controller design and its benefit prediction are based on the assumptions: brake and steer actuators continue to work normally after the initial impact; no malfunction occurs in the sensors used by PIC; no significant deformations occur in the vehicle body that the vehicle static weight distribution remains at its nominal value. This implies that the proposed function can be firstly applicable to the cars which were not involved in major damage after the first impact.
- Interaction between the controller and driver, e.g. driver overriding. Here it is assumed that driver hardly applies correct control to the steering and braking in the presence of relatively large disturbances, as following an external impact to the car body, i.e. autonomous vehicle actions are assumed for some seconds immediately after the first impact. Nevertheless, in reality, it is also possible that the driver would act to control the actuators him/herself.

1.5 Scientific contribution of this thesis

The main contributions of this thesis are in short:

- An in-depth analysis is conducted in an accident database: cars which have potential to gain safety benefits from PIC are identified; several representative accident cases are selected; post impact vehicle dynamics are analyzed via case-to-case study considering the overall accident scenario; benefit measures with respect to the vehicle dynamic states are determined for each case; it is found that reduction of *kinetic energy* and *path lateral deviation* would be beneficial under most post impact circumstances. See Paper A.
- A trajectory optimization scheme is developed to investigate the capability of influencing vehicle path after the first impact. The path control aims to minimize the maximum path lateral deviation using individual friction brakes at the four wheels. It is found that effective control across the very wide range of post impact kinematics can be significantly achieved by switching between three sub-strategies established on vehicle body level. There exists distinct discontinuities in the optimal response that multiple equilibria are found on the phase plane of dynamic states. The resulting interventions are found to be qualitatively different to classical ESC systems, and also to interventions proposed in other studies on post impact control which prioritize the minimization of any large post impact yaw rate. See Paper B.
- The potential benefits for reducing path lateral deviation are examined given the additional control of front axle steering angle, apart from individual wheel braking. The method of numerical optimization is adapted to determine the optimal controls for both actuator configurations. It is found that steering provides significant control benefits, though not for all post-impact kinematics. When steering is available, there exists an expanded range of kinematic conditions for which coupled control of yaw moments and lateral forces is the most effective control strategy. The sensitivity of vehicle response to the individual actuator controls is studied; it reveals this sensitivity is related to the actuator bandwidth and the lack of any dynamic cost in the longitudinal direction. This also motivates the further analysis including both the longitudinal and lateral dynamics in the cost function. See Paper E.
- A quasi-linear optimal controller (QLOC) is proposed to minimize the path lateral deviation provided the vehicle instability is suitably

bounded. The control performance compares favourably to the open-loop numerical optimization results. It uses optimal control theory to provide a semi-explicit solution of the path lateral control problem which includes the trade-off between global lateral force and yaw moment. The controller design method is novel in that it overcomes the limitations of applying model predictive control due to the nonlinearities of vehicle dynamics. It can be expected that the controller is also suitable to control vehicle path in other limit-handling circumstances, e.g. in crash-imminent scenarios to assist the driver to avoid collision. The applicability and robustness of QLOC is further confirmed by the design of a more computationally efficient control algorithm, and by testing on an independent high fidelity multi-body vehicle model. See Paper C and Paper F.

- A post impact path controller that incorporates the three sub-strategies for minimizing path lateral deviation is presented. It is also shown that friction adaptation may be implemented in a very efficient manner; the controller deals with different levels of road friction by scaling the dynamic variables from a fixed reference level. This approach provides an algorithm for adapting switching thresholds between the different components of the controller. It is verified that the controller can deal with a wide range of kinematics at different values of road friction. See Paper D.
- The crash risk for secondary collisions is formulated via a general cost function and an optimal controller is developed to minimize the prescribed cost. The cost function may penalize both longitudinal and lateral deviations from the point of initial impact, and is assumed to be a time-integrated quadratic function of position. For closed-loop implementation this formulation is further approximated using a simple terminal velocity cost, the direction of which represents predicted locations of maximum risk. A six-state quasi-linear path controller is developed using nonlinear optimal control theory; the controller is tested in example cases, verifying approximate equivalency between cost functions and satisfactory control performance compared with independent open-loop numerical optimizations. See Paper G.

1.6 Thesis outline

Part I serves as a résumé of this thesis. Chapter 1 mainly provides the background of this research work and deduces the research scope. A review of research related to post impact vehicle control is covered in Chapter 2, in terms of accident statistics, controller design and effectiveness evaluation. Chapter 3 summarizes the results from analysis of the German In-depth Accident Database, where the post impact vehicle dynamics problems are revealed and requirements on the control design are presented. The capability for reducing the post impact vehicle path lateral deviation from the original lane is investigated in Chapter 4; numerical trajectory optimization methods are applied to determine the optimal individual wheel brake and front axle steer control sequences, over a wide range of post impact vehicle kinematic conditions; a general form of the cost function with respect to the expected crash risk and severity is proposed. In Chapter 5, the design of a closed-loop algorithm for path lateral control is discussed; it involves the *coupled control* employing global lateral force and yaw moment simultaneously; an extended algorithm which considers both the vehicle longitudinal and lateral motions is also introduced. Based on the PIC-relevant cases found via accident analysis, several PIC function verification methods for driver interaction are investigated, see Chapter 6; a scheme of the function design for real-time implementation is discussed. Finally, Chapter 7 closes Part I with the conclusions and recommendations for future work. Complete versions of the papers discussed in the résumé are appended in Part II.

Chapter 2

Literature Review

Post impact vehicle dynamics control is found to be a rarely considered research field. However, in spite of the sparse literature, a number of papers have made progress with respect to accident statistics, control function design and evaluation methods of function effectiveness.

2.1 Statistics of multiple-event accidents

NASS-CDS (National Automotive Sampling System - Crashworthiness Data System) data from 1988 through 2004 show that every year in the USA, about 2.9 million light passenger vehicles are involved in tow-away crashes annually. Approximately 31% of these vehicles have at least one additional harmful event following the initial collision and the risks of both injury and fatality increase with the number of collision events [7].

Similar results were found by accident studies using other databases, e.g. Co-operative Crash Injury Study (CCIS) in UK (1992-2000) [3,22] and German In-Depth Accident Study (GIDAS) (1996-2000) collaborated between Medical University of Hannover and Technical University of Dresden; the proportions of MEAs were found to be 29.0% and 26.5% respectively for CCIS and GIDAS full-span dataset [23–25]. An accident analysis performed by the German Insurance Association additionally confirms that a vehicle involved in a *light* impact (e.g. the collisions with impact forces under certain thresholds) is more likely to experience a severe secondary collision, and about 33% of all accidents with severe injuries consist of MEAs [4]. The more severe the injury, the higher the share of MEAs [3]. It was also found that the probability and severity of a roll-over event is much higher as a consequence of initial impacts in MEAs, rather than as an isolated event in SEAs [26].

Furthermore, in order to understand how much benefit could be gained

by avoiding one or several *subsequent* impacts, the injury should be broken down into each event, apart from being treated as a total measure per accident. Specifically, in-depth accident analysis shows that approximately 50% of all MEAs-experienced passenger vehicles have the severe (i.e. AIS3+) injuries sustained in one or several subsequent impacts [6]. Other research work into the injuries sustained per impact during MEAs also concluded with similar statement although without giving a statically aggregated quantity [5, 27]. Nevertheless, these injury cost quantifications do not count the vehicle and passenger involved in such MEAs but with only one collision of its own; this means the injuries of a *third party* in each MEA are not studied in these MEAs analysis. This implies that it would be conservative to predict the benefits merely gained by the *host* vehicle which avoids or mitigates one or several subsequent impacts, since the benefits for *third parties* are not counted. This would require an “injury” measure which can be a sum of the injuries and damage for several involved parties, for instance “*functional years lost*” [28].

Above all, these studies mostly expressed the percentage of Multiple Event Accidents in one dimension, i.e. impact type, or in two dimensions, i.e. impact type and Maximum Abbreviated Injury Scale (MAIS), which are commonly used to evaluate the passive safety systems. Except for the *speed difference of collision partners* (Δv) used by Jing et al. [29] and Häussler et al. [30], none of the other studies above conducted the analysis concerning active safety systems design, i.e. no filtering of MEAs in terms of *vehicle dynamics variables* was considered.

2.2 PIC-relevant functions

Post Impact Control functions are to be considered closely related to the well-known vehicle dynamics control functions whose reference signals are mainly based on driver inputs, e.g. [13, 31]. In the recent decades, the rapid progress in sensing technology and its applications in the automotive industry has enabled the development of active safety systems which rely on information about the surroundings. These systems, in addition to driver inputs, start to derive the control reference from the road geometry and traffic scenarios, and apply control of the vehicle motion in the road coordinate system. Typical systems emerging on the market nowadays are Autonomous Emergency Braking (AEB), Adaptive Cruise Control (ACC), Lane Keep Assist System (LKAS), *City Safety*[®] etc., which are usually categorized as Advanced Driver Assistance Systems (ADAS). Also popularly investigated in academia are the lane-tracking and stability controllers especially for autonomous driving at limit-handling conditions,

e.g. [32–40], where high side-slip drifting dynamics and techniques are thoroughly analyzed; and collision avoidance systems during lane-changing and cornering manoeuvres for everyday driving have been extensively studied in e.g. [41–45].

As a pioneer to industrialize a PIC-relevant safety system, Robert Bosch GmbH invented the Secondary Collision Mitigation (SCM) system [19, 30] which automatically decelerates the host vehicle after an initial collision. It is designed by networking the airbag control unit with an ESC function, so that a secondary collision can be prevented or mitigated; SCM function retrieves information from the airbag system to calculate that an impact of a certain violence level has taken place and requests braking deceleration. This request is then sent to the ESC control unit which commands automatic braking using the Anti-lock Brake System (ABS). Further in [30], Häußler et al. demonstrated the potential benefits of SCM by simulation and real driving test on low friction road, where abrupt steering intervention and impulse from a steam rocket was respectively used to disturb the vehicle with the driver in the loop.

Salfeld et al. proposed a yaw moment optimization algorithm in order to reduce *yaw rate* in various skidding and spinning motions, via controls of the individual wheel brake slip and front axle steering angles [46, 47]. In [48], a nonlinear *predictive* controller was designed using the information given by a lane detection system instead of the driver steering angle; the controller uses active front steering actuator to correct the driver steering inputs that are improper under adverse driving situations, e.g. abrupt changes in road friction during cornering; it not only stabilizes the vehicle yaw motion and side slip angle but also the lateral motion with respect to the driving lane.

A vehicle collision model was developed by Jing et al. to characterize vehicle motions due to a light impact [49] and a crash sensing and validation scheme was proposed to activate the controller [7]. One stabilization controller which consists of an MPC-based supervisory stage, an intermediate stage for optimal control allocation, and wheel slip ratio tracking at the actuator stage, was developed to attenuate excessive vehicle *yaw rate* via differential braking. The overall system was evaluated in *CarSim*[®] [50] simulation model under a set of angled rear-end impacts [7]; its path control was achieved by first recovering stability and then allowing the driver to steer back to the road center.

Pettersson and Tidholm developed a stability controller *assist driver* to prevent a car from skidding in light side collisions [51]. It activates at slight lateral acceleration and vehicle speed, by proportional one-side braking to correct the errors of yaw rate and lateral acceleration, and by using proportional-derivative steering wheel torque superimposition to correct the

side slip error. Several cross-wind and side impact conditions were modeled to evaluate the controller in the driving simulator at Chalmers. Improvements from the original ESC controller in the simulator were presented in terms of less lateral displacement and yaw rate deviations, as well as better driver experience.

In the California PATH program [52], Tan and Chan also considered that a minor collision will not disable the actuators of a vehicle, and that a strategy of controlling the *vehicle trajectories* would mitigate the accident consequences significantly. There a feedback steering controller was developed using a linear model of the vehicle lateral dynamics; this controls the lateral displacement and yaw angle simultaneously by looking ahead on a straight or a curved path, where the controller parameters are tuned for specific vehicle models based on the calculated bounds of resulting lateral displacements. The post impact initial conditions were nevertheless limited to very mild cases, considering only rear-end collisions with small offsets.

2.3 Methods for ESC benefit evaluation

As mentioned above, Electronic Stability Control (ESC) system is pertinent to post impact control and its benefit evaluation methods have been well developed by both automotive industry and academia. Hence, a study on these methods may very well provide hints about how to predict the safety benefits of the PIC systems.

Since the implementation of ESC on the passenger cars in 1995, there have been numerous investigations about its benefit evaluation methods. Generally, the main scientific tools for the evaluation are: Field Operational Tests (FOTs) via naturalistic driving study [53, 54], driving simulator [51], simulations in Personal Computer (PC) using computational vehicle and driver model [55], on-track vehicle testing [56, 57], and last but not least, accident analysis [15, 16].

- For the simulation-based methods, one attempt was initialized to estimate the ESC efficiency *after* an initial collision in MEAs [51, 55]. A generic set of light side collisions were introduced at the height of mass centre. A *pass/fail* criterion on path lateral deviation was adopted both in the PC and driving simulator environment.
- FOTs collect a large amount of videos and vehicle kinematics data logged from highly capable instrumentation systems. Apart from the data that normally appear in an epidemiological accident database, video and electronic data of driver and vehicle performance are stored and classified by pre-event manoeuvre, precipitating factor, event type,

2.3. METHODS FOR ESC BENEFIT EVALUATION

contributing factors, and avoidance manoeuvre exhibited [53]. Parameters such as vehicle speed, vehicle headway, time-to-collision, and driver reaction time are also recorded. The primary goal is: *to provide vital exposure and pre-crash data necessary for understanding causes of crashes, supporting the development and refinement of crash avoidance countermeasures, and estimating the potential of these countermeasures to reduce crashes and their consequences*. In the 100-Car Naturalistic Study, data was collected during about 12 months on 100 cars, 82 crashes occurred and 69 of them have complete data recorded.

- On-track vehicle testing are mainly used by governmental authorities e.g. NHTSA, EuroNCAP, USNCAP and automobile manufacturers to set or satisfy the industrial standard for ESC-pertinent products. NHTSA investigated 12 manoeuvres with 12 steering combinations, such as J-turn, Fishhook, Pulse Steer, Sine Steer, Sine with Dwell, Yaw Acceleration Steering Reversal and so forth [56]. The performance evaluation criteria, sorted as the *pass/fail* method, usually have the benefit measures being yaw rate and lateral displacement at certain predefined time instant during one manoeuvre. However, these existing manoeuvres appear to be hardly able to cover all the types of vehicle motions that usually occur after the initial impacts in typical MEAs.
- In accident analysis, although different researchers used different definitions of *benefit* from a statistical point of view, *loss of stability* accidents were widely used as the base to perform the evaluation of ESC systems on-board. A popular benefit quantification formula is the division of two ratios: the numerator is the ratio between the number of *case crashes* and the number of *control crashes* for vehicles *with* ESC; the *denominator* is the corresponding ratio for vehicles *without* ESC [16]. The *case crash* is referred as the ESC-relevant crashes in which ESC is expected to be effective, whereas the *control crash* is referred as the ESC-irrelevant crashes in which ESC is expected to have no effect. Single-vehicle crashes or some subsets of those (e.g. loss of control) are often treated as “Cases”. “Controls” vary among studies that rear-end crashes, multi-vehicle crashes and a combination of crash types are mostly assigned [16]. The critical aspect of this method is to select cars that are identical in every other factor, but are only different in the presence or absence of ESC [15]. This is in reality very complicated since a lot of confounding factors exist, for instance, accident year span, car model year, where and how much the vehicles are driven, driver gender and age, driver driving habits

and physical conditions, ESC algorithms, and indirect influence from other safety systems on-board [16].

Above all, in the simulations and on-track vehicle testing, the criteria concerning certain vehicle dynamics variables of the *ESC-host vehicle* are used as benefit measures; while in accident analysis and FOTs studies, the human injury and vehicle damage *per crash* are mostly investigated. A direct linkage between these two types of quantities, which needs the information about accident scenes and their probabilities, is not found in any literature.

Chapter 3

Vehicle Dynamics after Impacts

3.1 Driver reactions after impacts

In everyday driving, the driver plays the leading role in controlling the vehicle motions in most contexts. In order to fully understand the pre-crash, crash and post-crash vehicle dynamics, apart from validated vehicle models, driver models are apparently of critical importance. As known, the driving behaviors at various crash-imminent events have been popularly studied previously, although well-adapted driver simulation models were hardly found [58]. Nevertheless, the knowledge about driver response *immediately after* crashes is rather limited due to the lack of information from accident databases. Drivers who are involved in accidents usually can not accurately remember what had occurred because of disorientation, panic and injuries. Hence, the good-quality data logged from naturalistic driving in FOTs projects are certainly of interests. However, the data analysis work is mostly focused on the evaluation and development of various informatics systems as the countermeasures to driver distraction and inattention, e.g. in the 100-Car study [53]; there the crash occurrence is so rare and minor that nearly no secondary impacts were recorded. Dozza has recently studied the factors that influence driver response time for evasive manoeuvres in real-world traffic, using the public 100-car and 8-truck naturalistic data from Virginia Tech Transportation Institute (VTTI) [59]; it shows even if the driver was able to see the hazard within his/her scope, the mean response time for car drivers there is 1.45 s, where lateral manoeuvres (steering) usually take extra 0.3 s more than longitudinal manoeuvres (braking). This result is found to be consistent to the ones discussed in [60].

In other studies, simulator tests were carried out where unprepared drivers were subjected to a simulated sudden side impact. Pettersson and

Tidholm found that driver response time can be as fast as 0.5 s there, and usually steering comes first before applying any brakes [51]. This might be because steering is relatively an easier task than braking; inertia forces due to impact could make it hard for the driver to responsively move foot from acceleration pedal to brake pedal. Here, in contrast to the results in [59] and [60], in simulator test the hazard is invisible and thus not sensed by the driver until the host vehicle is disturbed by the external impact; this may explain the immediate *steering* response by the driver in order to regain control of the vehicle as quickly as possible. Similar results were found in the work by Kusachov and Mouatamid, where the shortest steering response time was achieved by professional test drivers from the automotive industry [61]. Intuitively speaking, impact scenarios in a driving simulator can be easier for humans to handle than the real accident scenarios in which driver can become more disoriented, panicking or even unconscious, especially when the initial impact is so severe that airbag gets deployed. This will prolong driver reaction time with an unknown time delay, concerning the response selection and programming phase [60]. Under these circumstances, it is very possible that the driver will take none or incorrect actions in vehicle motion control. Further, on-track driving tests have revealed severe problems of incorrect actions even if the disturbances are slight, for instance, with abrupt steering intervention as “disturbance”; it was found that in the test, acceleration pedals were incorrectly pressed by most drivers [30].

3.2 Accident reconstruction

Above all, nowadays in-depth accident study is still the most popular approach to understand the causes of crashes. In the normal practice of accident analysis work, the subject vehicles trajectories are reconstructed so that they closely match the most important references, such as a sketch of accident scene with road layout, traffic situation, vehicle damage and especially brake marks. In this way, one can as well infer the driver reaction along with the sequence of an accident.

How to connect a sophisticated vehicle simulation model and a well-validated collision model is of key importance in order to accomplish the reconstruction properly. Numerous vehicle dynamics models [62, 63] and commercial software such as *veDYNA*[®], *CarSim*[®], *Dymola*[®] with vehicle dynamics library, *CarMaker*[®], *ADAMS/Car*[®] etc. are well developed for simulating vehicle motions in normal driving or during light disturbances, e.g. aggressive driver manoeuvre, cross-wind. Various computational models were also invented to simulate the vehicle collision mechanics and dy-

3.3. PIC-RELEVANT CARS IN REAL-WORLD ACCIDENTS

namics, for instance *PC-Crash*[®] using momentum conservation law [64,65], Newton's equations of motion correlating momentum with impulse [66], Brach's model with added tyre forces during *light* collisions [49] etc.; these models have different strengths and weaknesses concerning the trade-off between complexity and accuracy [67]. The *accident reconstruction* models are progressively being improved in order to take best account of both aspects: vehicle dynamics and collision mechanics. Previously, these models were poor in modeling the vehicle dynamics especially for pre-impact and post-impact motions, but focus more on the collision mechanics during impact. This weakness has been overcome recently by the implementations of more degrees of freedom vehicle model, tyre model, driver actions such as pre-impact braking, acceleration and steering etc. [68]. The enhanced reconstruction software used there, i.e. *PC-Crash*[®], has been tested in analyzing the accidents in the GIDAS database [69] during the past decade.

Hereby, in order to discover the dominating vehicle dynamics problems after impacts, the reconstruction data in GIDAS during July 1999 to June 2007 were analyzed. This includes reconstructed motions of 14600 passenger cars which correspond to 10200 accidents with at least one passenger car involved. Via filtering through a selected set of *search criteria*, cars which have potentials to gain safety benefits from PIC were identified. Furthermore, they were categorized and prioritized so that the representative cases were selected, whose post impact initial kinematics conditions were exported to the case-by-case simulations, see Paper A. The contents and updates of Paper A are briefly highlighted in the following section.

Figure 3.1 illustrates a scheme to predict the benefit of PIC system, by combining the results from accident analysis and vehicle dynamics simulations.

3.3 PIC-relevant cars in real-world accidents

As stated in the *Research Scope*, PIC-relevant is defined as that the host car of PIC function could expect positive safety benefits in multiple-event accidents. Accident analysis of these PIC-relevant cars, concerning both post impact vehicle dynamics and environmental factors was conducted in three steps below:

Identification Several *search criteria* are applied to identify the PIC-relevant cars. The criteria mostly consider the properties of vehicle stability control systems, including sensor and actuator capabilities, e.g. 1st impact is strong enough to be detected and the time to 2nd event is long enough compared to the actuator time delay. 995 cars

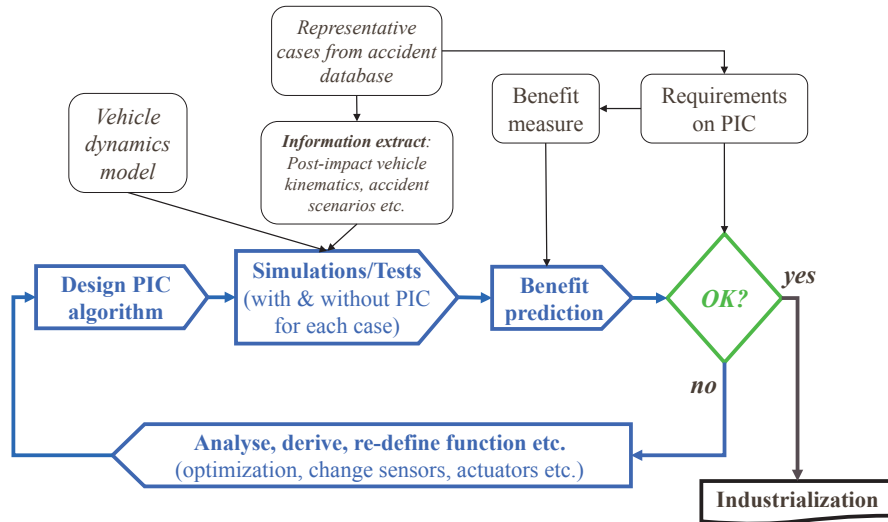


Figure 3.1: Methodology proposed for PIC benefit prediction.

are thus identified as PIC-relevant. If two of the criteria, i.e. sufficient dynamics ($v_0 > 15\text{km/h}$) and potential benefit ($v_{\text{PI}} > 20\text{km/h}$), are relaxed in order to include the **PIB**-relevant cars apart from the **PISC**-relevant ones in Paper A, the number of cars thus increases from 995 to 1063. Note that technology advances in braking and steering systems will certainly require updates on the search criteria used here, so that the number of cars that would benefit from PIC systems may increase.

Categorization The main challenge to categorize the relevant cars above was to determine the *critical parameters* which can together describe a post impact accident (i.e. case) scenario involving a PIC-relevant car and the values of these parameters are in good quality in the GIDAS database. In the end, *post impact velocity*, *post impact yaw rate*, *post impact side slip*, *impact area*, *road type* and *traffic scenario/road layout* were selected as the key factors. Post impact side slip angle is not provided in GIDAS, however an approximate method is found to estimate this angle from other three given quantities, and this estimation is verified by the reconstruction of sample cases [70]. At categorization, it was additionally considered that for cases where the post impact yaw rate is too high ($\dot{\psi}_{\text{PI}} > 150^\circ/\text{s}$) for using steering actuators alone, further use of the brake actuators is expected to help; this would then tighten the criterion: time to 2nd event, to be bigger than 0.6 s and thus the number of PISC-relevant cars was reduced from 995 to 944. This number corresponds to 0.14 million accidents

3.3. PIC-RELEVANT CARS IN REAL-WORLD ACCIDENTS

which could be affected in Germany during the aforementioned eight years.

Prioritization The combined frequency considering the five key characteristics factors above was calculated, so that 14 representative *chromosomes*¹ were prioritized. Within each chromosome group, one or two typical accidents were selected after scrutinizing additional database documents, e.g. photos, sketches, descriptions etc. In the end, the accident data of 17 type cases were collected for *benefit prediction* via the simulations.

Figure 3.2 shows the *problem space*² of the PIC-relevant cars, expressed as the properties of 1st impacts. Note that the total number of cases here is less than 1063, because several irrational cases recorded by the GIDAS data are washed out, e.g. an impact can not happen to the front part of the car but with impact angle as 30° . This picture shows that the 1st impacts of most MEAs occurred to the frontal of car body, or to the side from the front direction.

Figure 3.3 shows the *problem space* of the PIC-relevant cars, expressed as the *post impact* vehicle dynamics variables: yaw rate and side slip angle at CG. In [67, 70], the plots for the third dimension, i.e. post impact speed (v_{PI}), show that the dominant speed range is 20 – 80 km/h. The histogram in Figure 3.3 for PIC-relevant cars, shows the same pattern as the one previously found for PISC-relevant cars [67]: post impact yaw rates and side slip angles appear more near the low-amplitude regions, however the number of high-amplitude ones is not insignificant. It is also interesting to note that the cars were more exposed to negative yaw rates and negative side slip angles than the positive ones, which implies that the initial impulses more frequently occurred to the left-front part on the car body. This might be because of the right-hand traffic rule in Germany that vehicles are more easily hit by other vehicles from rear or on-coming ones from the left.

¹“Chromosome” is a term borrowed from gene terminology, since one representative scenario characterized by several factors is like a chromosome described by DNA.

²A real-world problem can be described in several dimensions. The space spanned by these dimensions is called a “problem space”. Here for avoiding secondary events, the problem space can be spanned of, for instance, 1st impact properties, post-impact vehicle kinematics, road friction, driver reaction time, distance to road edge etc.

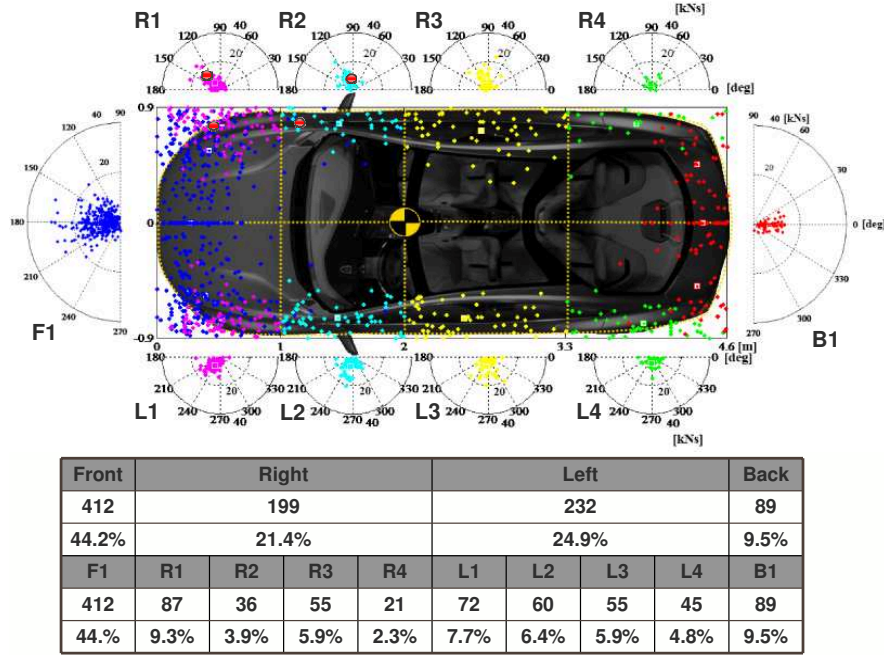


Figure 3.2: Problem space - expressed in 1st impact quantities [70]. The two large red dots represent Case 1 (forward) and Case 3 (behind) in Paper B.

3.4 Phase portrait and bifurcation characteristics

As shown in the *post-impact* problem space above, the vehicle would be placed at various positions in the state space after external impacts. It is interesting to visualize the vehicle system response on the phase plane. Hence, the vehicle side slip and yaw rate ($\beta, \dot{\psi}$) phase portraits are obtained by simulating a nonlinear 3-DOF vehicle model [71] at a fixed road wheel steer angle at the front axle δ_f . These nullclines are different from the normally defined *phase portraits* where longitudinal dynamics would not be considered. Here the vehicle initial speed is specified at 80 km/h, and initial yaw angles are determined by initial yaw rates which are assumed being linearly extrapolated from zero at the pre-impact instant. The post impact vehicle stability characteristics without active control can thus be illustrated.

Figure 3.4(a) below shows the fact that state trajectories in the neighborhood of the stable node $(0, 0)$ are attracted; while the states initiated outside the separatrix which divides the stable and unstable region on phase plane, will diverge away to infinity. This system behavior forms an unsta-

3.4. PHASE PORTRAIT AND BIFURCATION CHARACTERISTICS

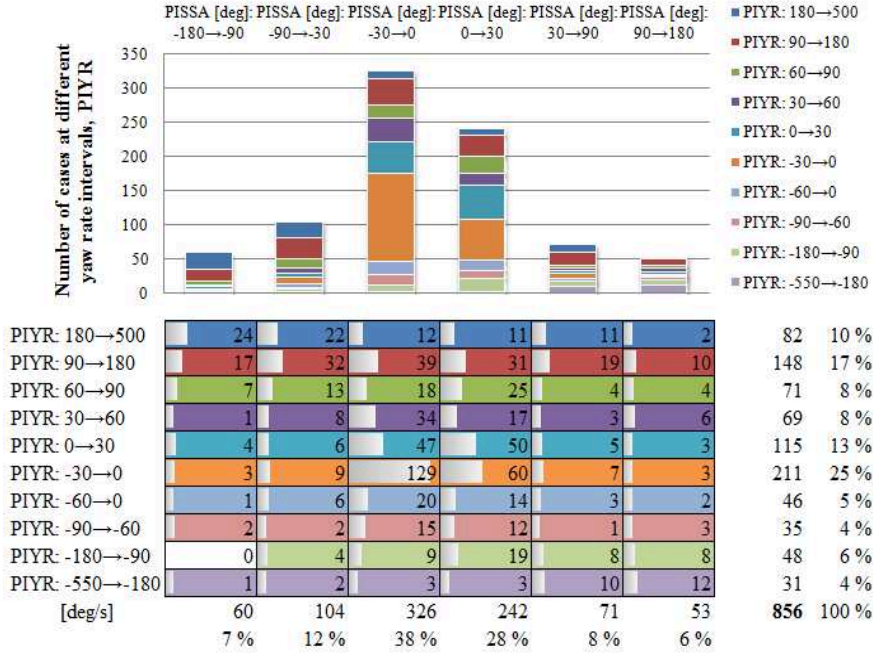


Figure 3.3: Problem space - expressed in *post* 1st impact quantities [70]. (PIYR: post impact yaw rate, PISSA: post impact side slip angle.)

ble saddle point respectively at 2nd and 4th quadrant which represent a left-handed and right-handed drift equilibrium (red dots in Figure 3.4(a)), i.e. no state converges to this equilibrium which actually corresponds to the steady state cornering condition associated with drifting manoeuvre commonly used by racing drivers [35]. However, as the constant road wheel angle is progressively increased in either positive or negative direction, the stable node migrates towards one of the saddle points and finally annihilate each other; simultaneously the other saddle point moves away from the y-axis, see one example in Figure 3.4(b). Considering δ_f as one parameter of the studied system, the qualitative change of equilibria positions and properties is usually called *bifurcation* and more specifically in our case here, “saddle-node bifurcation”.

The analysis above clearly shows that the nonlinear vehicle system can end up in the unstable region after impacts. The instability property is so sensitive to road wheel steer angles that it becomes even more difficult to control the vehicle if the wheels are steered to a wrong angle. In the emergency situation immediately after sudden impacts, drivers may tend to over-correct the steering wheel [30, 61]; thus the stable node disappears and the vehicle falls into the “black hole” of considerable side slip due to the bifurcation phenomenon. For instance, in Figure 3.4(b), the nullcline

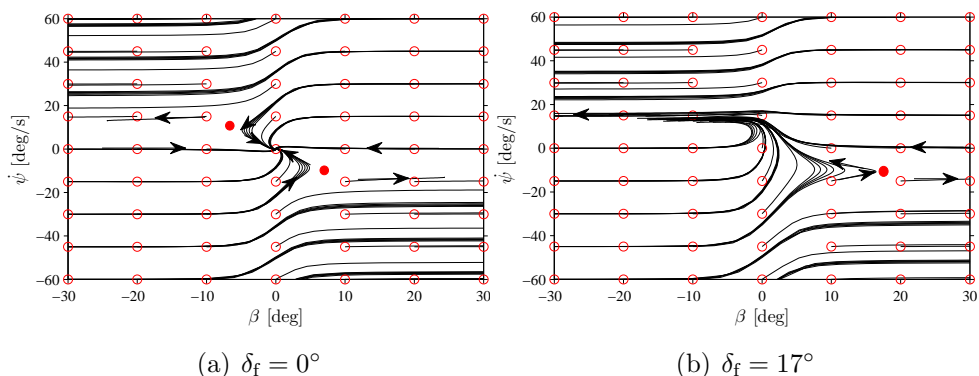


Figure 3.4: Phase portraits on low-friction surface. Red circles represent the post-impact initial states expressed as $(\beta_0, \dot{\psi}_0)$. $v_0 = 80$ km/h. Black arrows show the gradients of state trajectories near equilibria.

starting from $(-30, -30)$ in the phase plane, approaches but not resides at the $(0,0)$ point; instead it diverges with positive yaw and negative side slip due to the positive steer angle which stays longer time than it should be.

On the other hand, it is expected that certain feedback control algorithms will be able to expand the *stable region*. Nevertheless, usually brake and steer actuators have limits to generate fast and sufficient forces and moments. Hence there can be some post-impact kinematics which can not be stabilized in time, especially before the vehicle would have already left the safe zone, e.g. original travelling lane. To prevent the secondary collisions, the conventional concept of stabilization may thus be not the most effective countermeasure as the top control demand in the post impact control architecture; path control at the tyre limits appears to be more directly associated to the safety benefit of PIC system. Chapter 4 and Paper B have presented an example of how to obtain and to analyze the optimized path control sequences on phase plane, where three sub-strategies for minimizing the vehicle path lateral deviation were identified.

3.5 Case-by-case analysis

Having identified the representative cases, the vehicle dynamics after impacts were then analyzed via case-by-case simulations using a 3-DOF vehicle model. One on-market sedan model was chosen as the research vehicle to predict the benefit of PIC system, rather than copying the actual vehicles involved in each accident recorded by GIDAS. This research vehicle is considered as the representative of the future PIC function-host cars. It is

assumed that if this car was subjected to similar *circumstances* as the accident car, it would reach the same *post-impact* initial kinematics in the same recorded accident scenario. This approach of capturing the key information for *post* impact vehicle dynamics simulations is denoted as *information extract* phase in Figure 3.1 above. The comparison with and without PIC is thus expected to reflect the real-world safety benefits of the host vehicle. Two simple PIC algorithms were developed for applying the methodology as a first trial: (i) ESC-like one-side differential braking that corrects the errors of yaw rate and side slip angle; (ii) lock-front-axle braking that reduces front cornering stiffness and thus attenuates the oversteer tendency.

3.5.1 Causes of secondary events

The on-scene accident sketches and the simulation results were used to analyze the vehicle motion control problems causing 2nd events in MEAs. Phase portrait depicting the instantaneous yaw rate, lateral velocity and tyre side slip angles was as well used to show the vehicle instability in terms of loosing road grip on either or both axles, see details in Paper A.

Based on the stability criteria with respect to saturated friction at tyres, together with the vehicle dynamics and path plots, narrative descriptions on the traffic situation and other reconstructed parameters such as impact point, impulse angle, traveling distance and rotation between the 1st and 2nd impact etc, three causes of secondary events were identified, namely: *trajectory deviation*, *moderate instability* and *severe instability*. Individual case studies showed that kinetic energy, lateral deviation, yaw angle, yaw rate, front and rear axle side slip angle are closely related to the occurrence of secondary events. These six variables are also assigned as the benefit measures, combination of which can be formulated as a common measure, e.g. “functional years lost”. The common measure is not used in the present thesis but recommended for a thorough benefit and risk analysis during the function industrialization process.

3.5.2 Benefits evaluation using example controller

Simulations show that only for the cases where *trajectory deviation* were the main cause of 2nd events, it was efficient to avoid or mitigate the secondary collision by stabilizing the vehicle and *subsequently* assume that either the driver or any controller will steer back to the original lane. However for more severe post impact kinematic conditions (*moderate instability* and *severe instability*), yaw rate stabilization strategy hardly helped to reduce the excessive lateral deviation that leads to the subsequent impacts. In some cases, the lateral deviation was even increased with either *differential*

braking or *lock front* controls. In addition, it was noted that, as soon as the post-impact initial yaw rate and side slip go beyond a certain value, to immediately stabilize yaw rate will essentially make the side slip angle at global road coordinate worse. Please see Table 5 in Paper A for the details about each representative group of PIC-relevant accidents, regarding the cause of secondary events, the predicted benefits and the proposals of control variables.

In brief, through the studies of 17 type cases, the reduction of vehicle *kinetic energy* and *path lateral deviation* were found to be mostly beneficial for secondary collision mitigation. As discussed above, the real-world accidents covers a wide range of post-impact vehicle kinematics; at different intervals of such range, the most critical motion control problems and the corresponding countermeasures can be different. Therefore, in Paper A, a brief scheme of controller selection was proposed so that different controls should be activated at different phases during the 1st and 2nd impact. In order to identify and understand what are these effective controls, the optimal brake sequences for reducing the vehicle path lateral deviation were explored, see Paper B and Chapter 4 of this thesis.

Chapter 4

Optimal Control Synthesis

Accident statistics show, most secondary events in MEAs occurred due to excessive lateral deviation from the road or lane centre after an initial collision [2]; the secondary event may be a collision with a road-side stationary object or another moving vehicle at adjacent lanes, or it may be a rollover event. A previous study on the estimation of potential safety benefits gained from post impact interventions found that if lateral deviations were to be reduced, in many cases it is possible to mitigate or completely avoid secondary events [67]. Therefore, the ability to minimize the post impact path lateral deviation¹ can be greatly beneficial to road traffic safety, provided significant controlled changes in path are feasible.

Prior to the design of a controller that can minimize the lateral deviation during a certain time window after the initial impact, it is worthwhile to investigate the effectiveness of the on-board actuators by off-line trajectory optimizations. The numerical approaches for trajectory optimization appear to be diverse; Betts found that a great deal of them have been directed toward solving specific problems; what works well for one problem may be totally inappropriate for another problem [72]. Ross pointed out: while not exactly the same, the goal of solving a trajectory optimization problem is essentially the same as solving an optimal control problem [73]. Trajectory optimization is thus essentially about dynamic optimization of some performance measure within prescribed constraints and time horizon. In the following, optimization methods are briefly discussed and the general and specific optimization problems are formulated concerning different cost functions; optimal path control strategies are synthesized from the numeri-

¹Minimizing lateral displacement is not necessarily contradictory to reducing kinetic energy. After impacts, vehicle yaw rates and tyre side slips are typically large, hence the magnitude of tyre force vector does not change with its varied angle, see Figure 4.3 below. In this case, both translational and rotational kinetic energy can be efficiently reduced. A general optimization problem formulation is discussed in details in Section 4.4.

cally optimized brake and steer control sequences.

4.1 Optimization methods

Generally, the optimal control sequences with respect to a cost functional (J) can be obtained via solving the following dynamic optimization problem [74]:

$$J = \min_{\mathbf{x}(t), \mathbf{u}(t), t_f} \Phi(\mathbf{x}(t_f), \mathbf{p}) + \int_{t_0}^{t_f} L(\mathbf{x}(t), \mathbf{u}(t), \mathbf{p}, t) \cdot dt \quad (4.1)$$

s.t.

$$0 = e(\dot{\mathbf{x}}(t), \mathbf{x}(t), \mathbf{u}(t), \mathbf{p}, \mathbf{w}(t), t), \text{vehicle dynamic equations} \quad (4.2)$$

$$0 \leq c(\mathbf{x}(t), \mathbf{u}(t), \mathbf{w}(t), \mathbf{p}, t), \text{path and control variables constraints} \quad (4.3)$$

$$0 = s(\mathbf{x}(t_0), \mathbf{p}), \text{initial conditions} \quad (4.4)$$

$$0 = r(\mathbf{x}(t_f), \mathbf{p}), \text{final conditions} \quad (4.5)$$

where \mathbf{x} is the states vector, \mathbf{u} is the control inputs vector, \mathbf{p} is the parameters vector, \mathbf{w} is the vector of model uncertainties and disturbances, t_0 is the initial time instant while t_f is the final time; the terms Φ and L are respectively called the final time cost and Lagrangian.

On the topic of dynamic optimization methods, mostly common used nowadays in engineering practice are: dynamic programming (DP, i.e. principle of optimality) and nonlinear programming (NLP, i.e. nonlinear optimization). There exists a variety of numerical algorithms [75, 76] that are designed to iteratively solve the sub-problems arising from the ones formulated upon these two methods, especially in the cases where the original objective functions and constraints are large, nonlinear and complex. This is exactly the property of a vehicle system that is posed at high accelerations and velocities after external disturbance. Two classes of *direct* approaches to transcribe an optimal control problem to a non-convex constrained NLP problem are:

Sequential methods Popularly used are direct single or multiple shooting methods, where the controls are usually approximated by piecewise polynomials and the system dynamics is integrated throughout the entire time horizon at once or at several intervals; the solution of state profile in continuous time together with the discretized control profile are iterated using certain NLP solver, until optimal controls are found. This method tends to be computationally expensive since accurate integrator and thus long execution time are required. The NLP problem

is of infinite dimension here so that convergence is not so easy with respect to difficulties in the computation of gradients and Hessian of the Lagrangian, especially for large and complex dynamic systems. However, it works well with hybrid-event system, and relatively simple to implement using existing system models and optimization algorithms, e.g. MATLAB *fmincon* [77] and ACADO Toolkit [78].

Simultaneous methods Popularly used is direct collocation method, where both controls and states profiles are discretized. The system differential equation is hence approximated as a set of DAEs which enter the transcribed NLP problem as constraints; these constraints can be violated during the optimization but must be satisfied at the optimal solution. Since here large-scale sparse dimensional static NLP problems are solved in one step, it converges faster although requires more memory space in computer. This method generally handles large and complex system well, which is however expected to be as smooth as possible; on the other hand, the optimization problem is not necessarily convex for achieve the global optimum. While the programming platforms can be various for different optimization software packages using direction collocation method, e.g. MATLAB-based PROPT [79] and GPOPS [80], Modelica-based JModelica.org [81] and Fortran-based DIRCOL [82] etc., their NLP solvers all use most well-known open-source algorithms such as Interior Point OPTimizer (IPOPT) [83] and Sparse Nonlinear OPTimizer (SNOPT) [84].

4.2 Minimization of path lateral deviation

As stated above, the control target here is to reduce path lateral deviation after impacts. This post impact path control problem is further illustrated in Figure 4.1. In the thesis, the present trajectory optimization problem is solved using both the *direct single shooting* and *direct collocation* methods above, although the formulation of cost functions differ for practical reasons.

As a first attempt to solve the aforementioned large-scale and complex NLP problem for a vehicle system, it is important to evaluate and understand the influence of active chassis control on vehicle path at a high level. Hence the *direct shooting* approach is applied when it is necessary to overcome the possible discontinuity issues arising from excessive vehicle yaw motions, e.g. when the vehicle rotates beyond 90 degrees relative to the path and the longitudinal speed becomes negative. It is also necessary to keep the ODE system as simple as possible in order to achieve satisfied convergence, while still to deliver a relevant solution that properly describes the vehi-

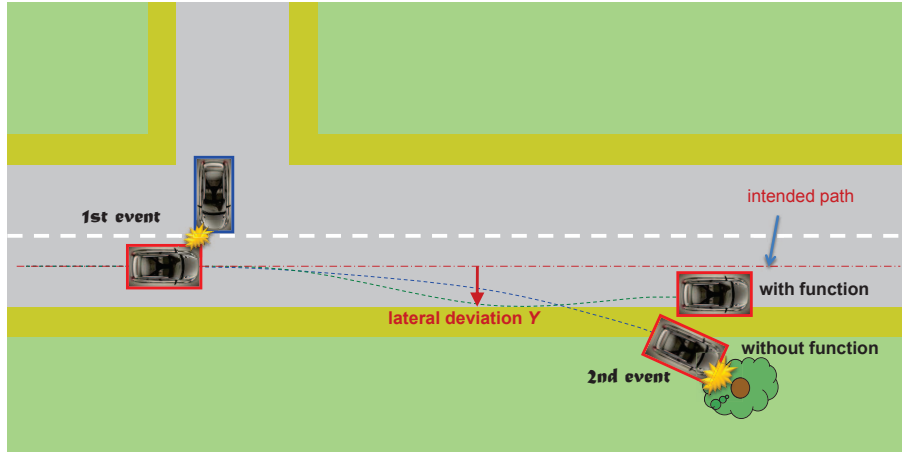


Figure 4.1: Illustration of a path optimal control problem that minimizes the lateral deviation from the intended path. Blue-framed: bullet vehicle, red-framed: host vehicle.

cle system. Therefore verification is done using more complex and higher fidelity vehicle model, by comparing the simulated state profiles given the same control sequences, more details about this verification are discussed in Paper B and Paper J.

In Paper B, it is assumed that the host vehicle is equipped with hydraulic brake systems which can apply friction brake control at each wheel. The individual-wheel brake modes are optimized using a 3-DOF vehicle model in the MATLAB function *fmincon* [77], which uses the default NLP algorithm as Sequential Quadratic Programming (SQP); this algorithm updates an estimate of the Hessian of the Lagrangian at each iteration by solving a quadratic programming subproblem. The objective function for optimization is chosen to be relevant to typical severity secondary events in an MEA occurring on a straight road. It is based on both the lateral deviation from the intended path and the time duration of this deviation [17]:

$$J = \sqrt[4]{\frac{\int_0^{t_f} Y^4 \cdot dt}{t_f}} \quad (4.6)$$

The 4-norm formulation over a fixed time horizon $t \in [0, t_f]$ is smoother and thus more favourable for better numerical convergence compared to minimize the non-smooth Y_{\max} directly in *fmincon*; it also provides a satisfactory approximation to the infinite-norm problem, i.e. to minimizing the maximum path deviation, see Paper B. Here t_0 in Eq.4.1 is assumed as zero, and a constant is predefined as t_f for feasible implementation of the direct

4.2. MINIMIZATION OF PATH LATERAL DEVIATION

shooting method mentioned above. The post-impact initial kinematics are used as the initial conditions $s(\cdot)$, while the control variables are bounded by the limitations of hydraulic brake systems such as hydraulic pressure, flow and dead time limits etc., which enter as saturation and rate constraints in the function $c(\cdot)$ above.

Whereas the formulation in *fmincon* is found to be rather efficient to capture the optimal solution given the nonlinearities of vehicle system after impacts, more complex vehicle model and more control variables increase the difficulty of NLP considerably. For instance, the convergence of *fmincon* is hardly guaranteed when active front axle steering actuator is added. In this context, the *direct collocation* method is expected to overcome this limitation of *fmincon*. With added steering actuator in a 6-DOF vehicle model, a Modelica-based open source optimization platform is applied. The platform is called JModelica.org (JM), which features one particular algorithm based on the collocation of finite elements and relies on the solver IPOPT for obtaining a solution of the resulting nonlinear programming [81,85]. It proves to be faster in reaching optimum than *fmincon* given the same optimization problem; it can handle higher degree of freedom vehicle model with respect to both state and control variables; it does not find optimum if hybrid events, even if approximated with continuous functions which are smoother, occur to the vehicle model, e.g. tyre longitudinal velocity switches sign.

In JModelica.org, apart from the friction brakes power limits, the electric motor power limits for the Electric Power Assist Steering (EPAS) system is added as the actuator constraints. Furthermore, the minimum and maximum road-tyre normal forces (to avoid non-physical effects during potential wheel lift) are directly modeled as inequality constraints, together with the ones of limited road friction forces at certain tyre normal loads. Regarding the initial guess selected for the optimizations, the optimal solution is firstly identified for one PI kinematic condition starting from multiple arbitrary control inputs sequences; then as a small change is applied to this PI condition, the derived optimal control sequence is used as the initial guess for the next optimization; this process is continued for subsequent optimizations.

The cost function in JM is formulated as a terminal cost with *final* time t_f defined at the maximum lateral deviation (Y_{\max}):

$$J = Y_{\max}^2 = Y(t_f)^2, \text{ where } \dot{Y}(t_f) = 0. \quad (4.7)$$

This is a typical free-time optimal control problem where t_f is not known beforehand; therefore t_f is also specified in the initial guess of the optimization, in addition to the control inputs.

4.3 Optimal vehicle-level control strategies

The results from numerical optimizations have been able to reveal the interesting mechanisms of how to optimize the vehicle path laterally, at various post impact kinematic conditions. In general, it is found that no single simpler control mode (e.g. yaw motion control or locked-wheel braking) is optimal in reducing lateral deviations. Instead, within one accident, dynamic switching between a combination of these modes appears to be necessary. Taking brake-only actuation as an example, after higher amplitudes of yaw disturbances, if the yaw rate and side slip angle have the same sign, a locking of all four wheels gives lateral deviation close to being optimal; on the other hand, if they have the opposite sign, free rolling wheels gives the best approximation to the optimum. If the vehicle is mildly disturbed in yaw motion, the yaw moment plays an important role in regulating the dynamics; in fact, the yaw moment control here is different from the classical ESC interventions in that it applies a yaw moment which does not always oppose the vehicle rotation, e.g. the yaw moment remains negative for some time after the yaw rate passes through zero towards being negative. Section 3 in Paper B provides for the illustrations and more detailed explanations of the comparisons among single simpler control modes and the optimal strategy on vehicle force level.

4.3.1 Phase plane analysis

As mentioned above, single actuator control modes comprise certain approximation to the optimal strategy. However, these modes exist at different phases of the entire post impact control sequence, see Figure 17 in Paper B. In order to understand how the brake actuation and thus the vehicle-level dynamic behaviours emerge and to better characterize the general operation of the optimal controller, attention is turned onto the resultant forces and moments acting on the vehicle.

We consider a sweep of post-impact initial yaw rates $\dot{\psi}_{PI}$ and side slip angles β_{PI} . There the phase portraits are populated with several vehicle-level control modes, and three of them have been identified as dominating and thus critical for optimal path control, see the list below. Before describing these three strategies, it is important to define three types of forces and moments which are studied throughout this thesis: global longitudinal force F_{xg} , global lateral force F_{yg} and yaw moment M_z , i.e.

$$F_{xg} = \sum_{i=1}^4 (F_{xi} \cdot \cos\psi - F_{yi} \cdot \sin\psi) \quad (4.8)$$

$$F_{yg} = \sum_{i=1}^4 (F_{xi} \cdot \sin\psi + F_{yi} \cdot \cos\psi) \quad (4.9)$$

$$M_z = \sum_{i=1}^4 (F_{xi} \cdot d_i + F_{yi} \cdot l_i) \quad (4.10)$$

where g denotes *global* direction aligned with the intended path, F_{xi} and F_{yi} are respectively the tyre longitudinal and lateral forces in vehicle coordinates, ψ is the yaw angle relative to the intended path; d_i and l_i are the distance vector based on vehicle track width and wheelbase.

Lateral Force Control For severe initial rotations, global lateral force is maximized at every instant in the direction opposing harmful lateral deviations, irrespective of the yaw moment. Section 4.3.2 below shows the analysis of an example case.

Yaw Moment Control For less severe yawing, or after the vehicle rotation has slowed down, yaw moment control becomes important which has essential trade-off with favourable global lateral force. Section 4.3.3 below shows the analysis of an example case.

Settling Control After the maximum lateral deviation is reached, a settling motion takes place that involves synchronized contribution from lateral force and yaw moments, which are *not* on the friction limits but track a linear reference trajectory in a suitable phase plane.

As shown in Figure 18 and 19 in Paper B, an interesting character of the phase portrait can be summarized at vehicle force level: for small initial yaw rates, the initial response is dominated by *yaw moment control*, and the vehicle settles with a zero yaw angle. Beyond a certain threshold however, the initial response becomes *lateral force controlled*, while switching afterwards to the stabilizing pattern and settling into a reversed vehicle orientation ($\psi \approx 180^\circ$). As the initial yaw rate increases further the rotation goes beyond 180° , tending towards a full 360° rotation. These qualitative changes in yaw angle during settling occur suddenly as $\dot{\psi}_{PI}$ smoothly increases, giving a *discontinuity* in the overall system optimal response; such different responses result in *multiple equilibria* which are commonly seen in nonlinear dynamics, e.g. [86], but here occur because of discrete changes in preference for the optimal control. The analysis is shown in Section 5.3 of Paper B. This feature was further confirmed by Kim et al., via directly penalizing both vehicle lateral deviation and heading angle in numerical optimizations, where multiples of 180° heading was considered to be good for stabilizing a struck vehicle [87].

The strategies identified above with brake-only controls are found equally applicable to the configuration with additional steering actuators. This is not surprising if one notices that the optimal controls are studied via the total vehicle forces and moments which are aggregated by the individual tyre forces; control authority is enhanced by adding further actuators and the control performance in terms of Y_{\max} is therefore improved. However, the inclusion of additional actuators does not affect the underlying mechanism of applying optimal path control at the vehicle force level. In Paper E, as an example of exploring the improved cost with added steering control, Y_{\max} is compared over a set of post-impact yaw rates ($[-2.5, 0.5, 2.5]$ rad/s) at fixed PI side slip (15 deg), speed (15 m/s) and yaw angle (0 deg assuming short-duration impacts), see Figure 4.2 below. Note that the active front axle steering actuator is modeled to include realistic power limit of the electric motor in the EPAS system.

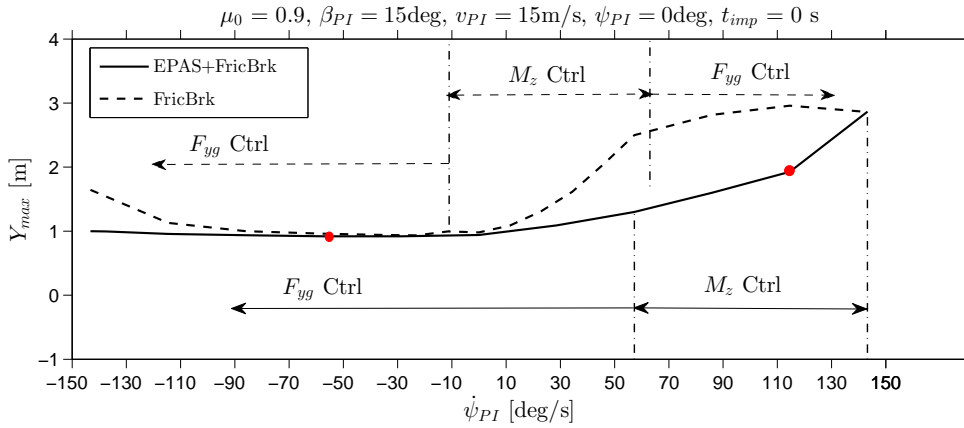


Figure 4.2: Maximum path lateral deviation with and without EPAS (both with individual-wheel friction brakes), given different post-impact yaw rates. Red dots represent the two example cases in Table 1 in Paper E.

It is interesting to note that the added benefits from the steering actuator vary at different PI conditions. At mild negative PI yaw rates, the maximum lateral deviation is the same with the two actuator configurations; as further discussed in one example (case 2) in Paper E, this is because for this type of post impact kinematics, no active steering control is necessary for achieving minimum Y_{\max} . As the PI yaw rate becomes more negative, steering becomes increasingly beneficial again. On the other hand, as the PI yaw rate becomes more positive, the added benefit of EPAS increases and then declines at large yaw disturbances.

4.3.2 Lateral force control

This first dominating strategy was found as *lateral force control*, which instantaneously selects brakes to achieve the maximum force opposing the vehicle lateral motion in the road global coordinate, i.e. F_{yg}^* in Figure 4.3.

Figure 4.3 below shows an example of the analysis of individual tyre forces and their contributions to the global lateral force F_{yg} .

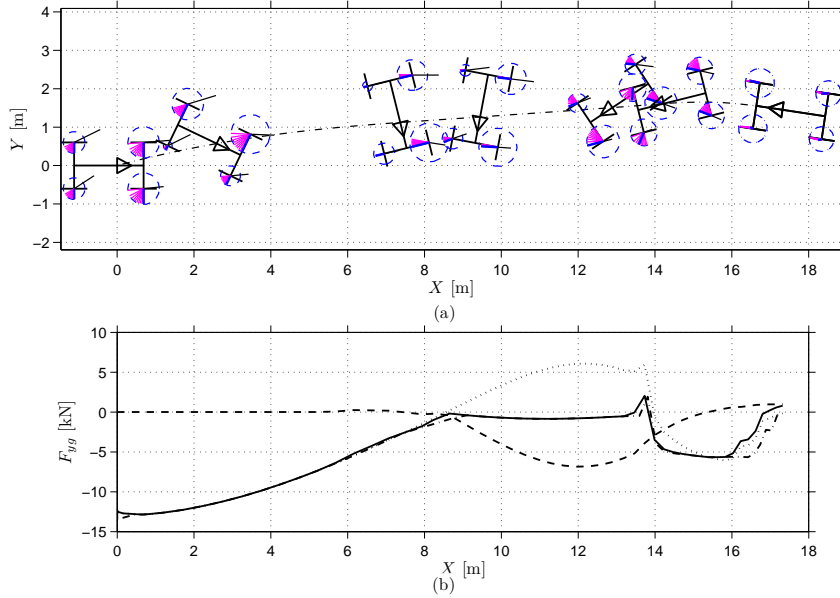


Figure 4.3: One example of *lateral force control*, (a) Optimal path and tyre force vectors. (Bold blue: optimal tyre force, thin black: tyre velocity, thin purple: available tyre forces, dashed blue: friction circle). (b) Global lateral forces. (solid: resultant lateral force F_{yg} , dash-dot: F_{yg}^* , dashed: tyre longitudinal force contribution, dotted: tyre lateral force contribution.)

The vehicle in this case was struck behind of CG so that exposed to post-impact states: $v_{PI} = 15$ m/s, $\beta_{PI} = 15^\circ$, $\dot{\psi}_{PI} = -143^\circ/\text{s}$. In plot (a), we can see, for $0 < X < 14$ m the tyre forces (solid blue) orient to instantaneously maximize F_{yg} . Plot (b) shows F_{yg} (solid line) tracks F_{yg}^* (dash-dot line) very accurately; additional information is shown in the dashed and dotted curves, which respectively indicate the contribution to F_{yg} from the longitudinal and lateral forces at the tyres. For this case, the free-rolling mode persists for $0 < X < 8.5$ m as all the corrective forces derive from lateral tyre forces. Other interesting cases and rather close observations on the pattern of tyre and global forces are presented in Section 4.1 of Paper B.

4.3.3 Yaw moment control

Another dominating optimal control strategy is described as *yaw moment control*, where global lateral force does not achieve its full capacity and yaw moment plays a more important role. In this situation there appears to be a dynamic trade-off between F_{yg} and M_z . This yaw moment control strategy is able to quickly limit both yaw velocity and side slip angle close to zero values, something that the *lateral force control* strategy never does.

To explore utilization and trade-off involving F_{yg} and M_z , a “cloud plot” of available forces and moments is presented. The available forces and moments are shown as a dark “cloud” (scatter plot) in the $F_{yg} - M_z$ plane as the individual brake torque inputs are varied; this brute-force method was presented previously in [88]. Here one example is investigated: the vehicle experienced a light impact forward of CG that created a milder yaw disturbance than the case above, $\dot{\psi}_{PI} = 57^\circ/\text{s}$. The cloud plot, Figure 4.4, shows this example as a case of yaw moments dominating the character of the optimal response, but *not* simply providing a yaw stability function. The cloud plot also shows another basic feature, at least during the early and critical stages of the response when $Y(t)$ is increasing: the selected point is on or near the left boundary of the cloud, whether or not it is the leftmost point.

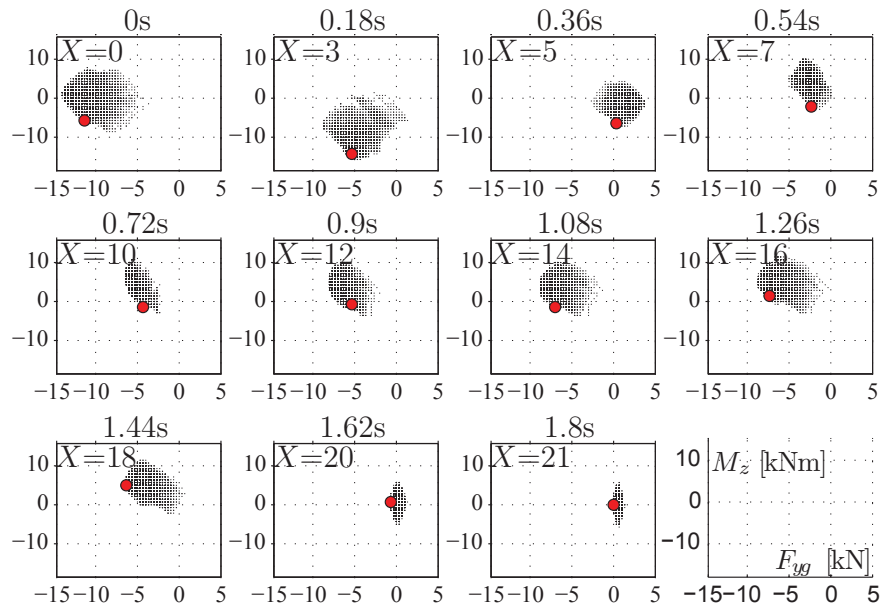


Figure 4.4: One example of *yaw moment control*, the attainable global lateral force F_{yg} and yaw moment M_z . The red circle shows the optimal choice.

4.4 Generalization of cost functions

As stated, the overall aim of PIC function is to attenuate the crash consequences associated with post impact motions, i.e. crash risk and severity are to be minimized. Although in general this is a very complex multi-objective optimization problem, it may be formulated as a cost function of the form:

$$J_1 = \int_0^{t_f} f_1 \cdot f_2 \cdot dt \quad (4.11)$$

where t_f is a time horizon for control, e.g. defining the time after which the risk for secondary event is expected to be largely diminished. This generalizes the cost function $J = Y_{\max}$ considered in earlier research. Function f_1 describes the expected injury and damage, which is typically characterized by the collision part, i.e. collision angle and relative velocity between two collision partners. Function f_2 represents collision probability per unit time, and it depends on the road layout and the surrounding traffic. Here the secondary collision risk is formulated as an exponential function of displacements; this is to assume the risk is described as isolines centered at the initial collision position:

$$f_2 = a \cdot X^n + b \cdot Y^m \quad (4.12)$$

which together define the deviation from the point of initial impact; in this case a and b indicate the relative risk of moving in X and Y directions; the exponents n and m describe the built-up pattern of collision risk as either X increases *or* Y increases. Note that, the isoline can be comprised of several parts with varying sets of n and m , for instance, the risk of collision from the traffic behind can be different to the one from traffic in front of the host vehicle. In an extreme case where only Y cost is concerned, we can define $f_2 = Y^{2m}$ where the risk isolines become lines symmetric and parallel to the X axis; this implies the risk ascends exponentially with increasing lateral deviation from the initial collision position; this special case is applied in Paper B.

If one considers that the crash risk does not start to increment until a certain distance from the collision position, the smallest possible area of such isoline can be defined as *field of safe travel*, which is a concept introduced in [89]. Figure 4.5 shows one scenario where curved road and oncoming traffic forms the boundary of safe travel area. Apparently the road geometry, traffic and also the position of host car are changing along time, therefore the *field of safe travel* and the risk isolines evolve dynamically as time goes by.

Note that for passenger vehicles with higher centre of gravity, e.g. SUV, the lateral accelerations can also enter as an important cost which poses

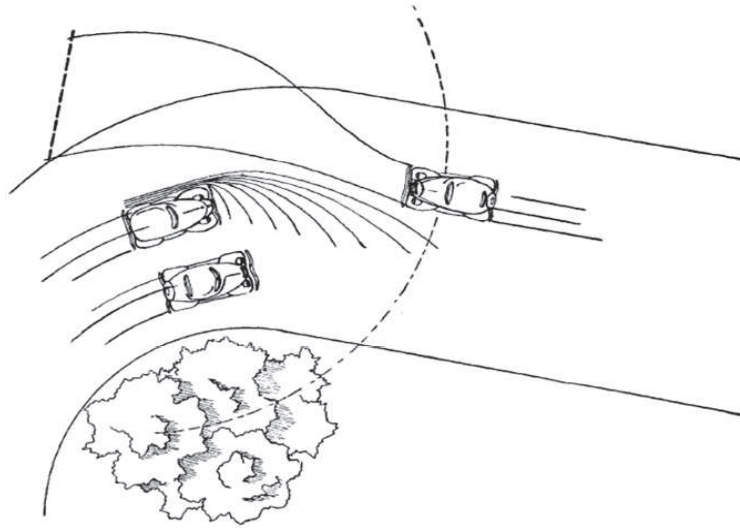


Figure 4.5: Field of safe travel predicted by driver or active safety systems on-board [89].

more danger of roll-over. This risk is related to controlling the lateral acceleration and thus the roll motion; the arbitration with roll-over mitigation functions is not explicitly considered in the present thesis.

4.4.1 Cost functions for crash risks

Here attention is restricted to collision probabilities, and we assume that crash severity is a constant. Hence define $f_1 = 1$ and further set $m = 2, n = 2$. The cost function that accounts for crash risks becomes:

$$J_{\text{risk}} = \int_0^{t_f} (a \cdot X^2 + b \cdot Y^2) \cdot dt \quad (4.13)$$

where $\dot{X}(t_f) = 0$, the ratio a/b is from 0 to infinity that it represents a continuous spectrum to bias relative contributions to crash risk arising in the X and Y directions. Figure 4.6 below shows the family of optimal paths with J_{risk} defined above; here the post-impact kinematics are the same as for the impact case discussed in Section 4.3.3. The actuator configuration is friction brakes plus EPAS. Both velocities \dot{X} and \dot{Y} reach zero at the end of control sequences. The optimal trajectories are found to be continuous although not linearly proportional to the ratio of weighting factors in the cost function.

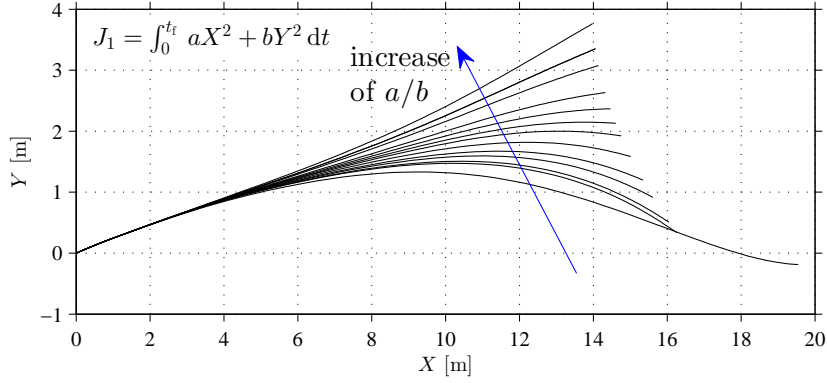


Figure 4.6: Optimal paths using cost function J_1 , with $f_1 = 1$ and $a/b \in [0, +\infty]$. The vehicle reaches full stop at the end of each trajectory.

4.4.2 Cost functions for crash severity

As stated in Chapter 3, the less the kinetic energy at the point of imminent secondary collision, the less the severity of the MEAs overall. Hence, the same optimization method is applied to minimize the costs associated with the kinetic energy W_k . Here for simplicity, only the translational part of W_k is used to define the intruding speed of two collision partners, e.g. a moving vehicle with stationary road-side obstacles:

$$W_k := v_x^2 + v_y^2 \quad (4.14)$$

The cost function is then intended to reduce the host vehicle speed at certain critical points, e.g. the road boundaries which are assumed to be the locations of impending collisions. It is assumed that rotational kinetic energy contributes little to the crash severity, i.e. at the vehicle collision part, the speed component which is contributed by the rotation is tangential to the collision force direction. Two variants of cost functions are compared below and here f_2 enters as a *constraint* instead of a *cost*. Considering only f_1 in the cost, Eq. 4.11 becomes:

$$J_{severity} = \left(\int_0^{t_f} \dot{v}_x \cdot dt \right)^2 + \left(\int_0^{t_f} \dot{v}_y \cdot dt \right)^2 = v_x^2(t_f) + v_y^2(t_f) \quad (4.15)$$

where f_1 includes two parts concerning kinetic energy at both x and y directions. Specifically for two different path constraints:

$$\begin{aligned} \text{(a)} \quad & J_{W_k} = v_x^2(t_f) + v_y^2(t_f), \text{ where } Y(t_f) = 3 \text{ m.} \\ \text{(b)} \quad & J_{W_k} = v_x^2(t_f) + v_y^2(t_f), \text{ where } Y(t_f) = 2.7 \text{ m.} \end{aligned} \quad (4.16)$$

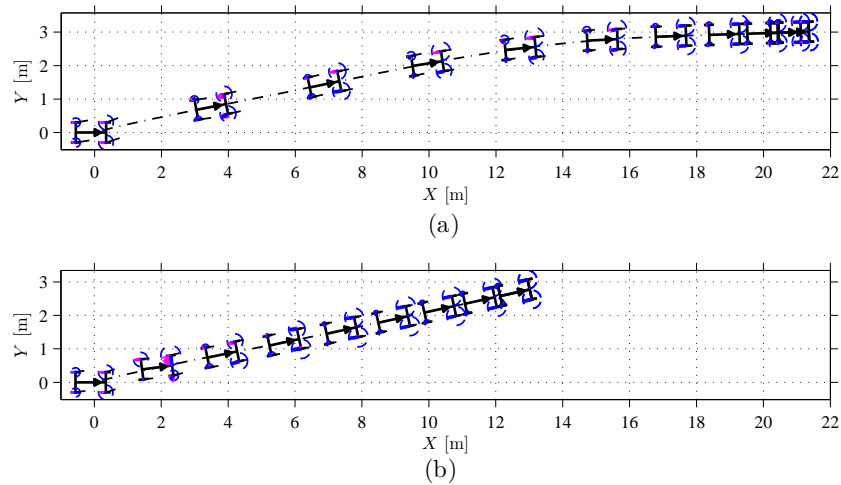


Figure 4.7: Optimal paths using the cost functions describing kinetic energy at two types of road boundaries: (a): $Y(t_f) = 3$ m, (b): $Y(t_f) = 2.7$ m. Actuator configuration: brake-only. (Bold blue: optimal tyre force, thin black: tyre velocity, thin purple: available tyre forces, dashed blue: friction circle.)

It is interesting to notice the different optimal trajectories arising from the different road boundary conditions, see Figure 4.7: if the road is relatively wide, it appears wise to firstly minimize the lateral deviation within the boundary and subsequently to reduce the longitudinal velocity until full stop; while if the road is narrow, full braking is applied nearly throughout the whole sequence until the vehicle hits the boundary, except at the very beginning when tyre side slip is so large that the lateral tyre forces opposing lateral displacement can reduce kinetic energy as efficiently as brake forces.

Future work remains to further generalize the cost functions for crash severity which will additionally account for other contributing factors, e.g. yaw angle and collision partners. The two exemplar cost functions above indicate that two approaches of formulations can be equivalent as the measure of overall crash consequence: crash risk as cost whereas severity measure as constraint, as shown by the optimal strategy resulted from variant (a) in Eq. 4.16; crash severity as cost whereas risk measure as constraint, as shown by the optimal strategy resulted from variant (b) in Eq. 4.16. This concept suggests more freedom to simplify cost functions, and thus to significantly ease the off-line numerical optimizations, as well as the design of on-line optimal controller.

Chapter 5

Optimal Post Impact Path Controller Design

The control synthesis, in Chapter 4, is useful for identifying and understanding the optimal control strategy, but there the numerical optimization of control signals was performed off-line, and is necessarily approximate and also infeasible for real-time implementation due to the high computational requirements. While the sub-strategy *lateral force control* is simple enough for direct implementation on a vehicle, the *yaw moment control* which involves trade-off between lateral force and yaw moment is not in a practical form for real-time application. In this thesis, the closed-loop form of the controller minimizing the aforementioned cost functionals is developed and compares favourably with the results of open-loop numerical optimization.

5.1 Optimal path control methods

In the recent decades, numerous studies have been done concerning optimal vehicle path control under different driving circumstances. Nonlinear Programming (NLP) is popularly applied on-line for driver modelling which usually involves using information of the reference path ahead of vehicle, i.e. preview or model predictive control. At each sample time, the NLP problem can be large and complex that convergence to the global minimum appears to be either infeasible or lengthy. Hence, both nonlinear model predictive control (NMPC) theory and linear optimal preview control theory are developed and implemented for this control purpose, based on a special case of nonlinear optimal control problem: Linear Quadratic (LQ) optimal control problem [34, 90–92]. The ultimate goal of the linearization is to achieve a sufficiently accurate optimal solution with reasonable and feasible computation speed for the real-time closed-loop control. Similar

to the *direct collocation* used in off-line numerical optimization, the vehicle model is firstly discretized so that the LQ programming is in finite dimension (sparse although large). Eq. 5.1 below presents such LQ problem with the cost functional concerning both tracking accuracy and control effort [93]:

$$J = \sum_{k=0}^n (\mathbf{x}^T(k)\mathbf{Q}\mathbf{x}(k) + \mathbf{u}^T(k)\mathbf{R}\mathbf{u}(k)) \quad (5.1)$$

where \mathbf{Q} and \mathbf{R} are respectively the weighting matrices of the control performance measures: tracking accuracy (presented by \mathbf{x}) and control effort (presented by \mathbf{u}). Given the constant weight matrices (\mathbf{Q} and \mathbf{R}), the state feedback of the linear time-invariant optimal control (i.e. $n \rightarrow \infty$, conventionally called LQR) can be found by solving the standard algebraic Riccati equation associated to the system state space model.

For applying the linear optimal preview control theory online, beforehand, the dynamic equilibrium are usually found and stored off-line via simulations of different manoeuvres. This type of equilibrium is called the set of “trim states” in [34], around which small perturbations are done in order to obtain the linearized models for solving the linear optimal preview path control problem on-line. Hence the “trim states” are crucial for providing the correct linearized models for LQ operation in the closed-loop control system; otherwise the tracking performance is certainly deteriorated and vehicle instability may incur, as shown in [34]. This implies that the predefined path is critical information for applying this method, especially at limit handling situations. However, as noted before, after an impact the vehicle can be operating at highly uncertain and extreme dynamics, such that prediction of an exact optimal path becomes not obvious. Furthermore, unlike the situation where there exists an intended and feasible path, the optimal choice of preview horizon is less intuitive if the optimal path and the corresponding time duration is unknown. For instance, if one selects to minimize the maximum of a path measure, e.g. lateral deviation, a challenge exists with respect to the estimate of the time instant at which this “maximum” happens, namely t_f ; this then increases the difficulty of selecting suitable amount of preview points, which directly affects the preview gains. In brief, linear preview control appears to be not well applicable to optimizing the *post impact* vehicle path.

For applying the NMPC theory online, the nonlinear vehicle model is often successively linearized along the predefined path, or more specifically, the state trajectory. The resultant linear models are then used in solving the *finite horizon* LQ programming at each sample time. Generally, increasing the prediction horizon will gain improvements in tracking and reductions in control magnitude [90]. However, since the locally linearized model is

used to predict the system response over the optimization horizon, conflict appears between the desired longer prediction horizon for making best use of the preview information and the fidelity of the linear model at current sample time being close to the nonlinear model in future time steps. As shown in [90], the control effort can become large and oscillatory using linearized models. Some comparisons of NMPC with the proposed quasi-linear optimal path controller are discussed in Section 5.2 below.

It is worth mentioning that given the nonlinear properties of the system, the system stability is checked via simulations concerning model uncertainties, after the control design using either of the two preview control methods; that is to say the focus here is on optimality while robustness is not considered at the primary phase of controller design. It is also interesting to note that unstable response was observed if actuator rate limits are not properly included as the constraints of the formulated optimization problem [34, 90, 91].

As known, not only direct methods such as NLP discussed above, but also the indirect method derived from *calculus of variations*, i.e. *Pontryagin's Maximum Principle* can be applied for solving nonlinear optimal control problem. The indirect approach requires to solve the dynamic equations of states and co-states either analytically or numerically; the ensuing two-point or multi-point boundary value problems are usually ill-conditioned and thus difficult to solve. This challenge is nevertheless expected to be considerably simplified if the tyres are at friction limits and the controls can be formulated as linear in the system equations. In the following, a semi-explicit approximation for optimal post impact path control is proposed, based on the *Pontryagin's Maximum Principle*. The essential details of the controller and the application to a wide range of post impact kinematics can be found in Paper C, Paper G, Paper D and Paper F.

5.2 Quasi-linear optimal controller

5.2.1 From optimal control theory to path control problem

The controller aims to limit the path deviation in the road coordinate system; thus for the purpose of controller design, the velocity variables are transformed from vehicle coordinate into global components: $\mathbf{x} = [X, \dot{X}, Y, \dot{Y}, \psi, \dot{\psi}]^T$. We also transform from actuator inputs $\mathbf{u} = [F_{w1}, F_{w2}, F_{w3}, F_{w4}]^T$ to the resultant vehicle body forces and yaw moments: $\tilde{\mathbf{u}} = [F_{xg}^{\text{act}}/m, F_{yg}^{\text{act}}/m, M_z^{\text{act}}/I_{zz}]^T$. Here *act* denotes that we consider the *active* contributions from braking torques and steering angle inputs relative to their passive values, i.e. rel-

ative to $\mathbf{u} = \mathbf{0}$. Each braking torque is transformed to the braking force at the corresponding tyre-ground contact patch F_{xwi} which determines F_{xi} and F_{yi} via the tyre model [71] and hence $\tilde{\mathbf{u}}$ is found.

After these transformations, the vehicle dynamical system equations can now be written as:

$$\begin{aligned}\dot{\mathbf{x}} &= \mathbf{f}_0(\mathbf{x}(t)) + B \cdot \tilde{\mathbf{u}}(t) \\ y &= C \cdot \mathbf{x}\end{aligned}\tag{5.2}$$

$$\text{where: } B = \begin{bmatrix} 0 & 0 & 0 \\ 1 & 0 & 0 \\ 0 & 0 & 0 \\ 0 & 1 & 0 \\ 0 & 0 & 0 \\ 0 & 0 & 1 \end{bmatrix}, \quad C = [0 \quad 0 \quad 1 \quad 0 \quad 0 \quad 0].$$

A quasi-linear optimal controller (QLOC) is then developed using non-linear optimal control theory. The controller is *quasi-linear*, since it combines the linear co-states dynamics and nonlinear constraints due to tyre friction limits. Firstly the cost function J is kept to *minimize the maximum lateral deviation from the original path*, here for convenience, as a quadratic function:

$$J = \frac{1}{2}y_f^2 = \frac{1}{2}Y_f^2 = \frac{1}{2}Y_{\max}^2\tag{5.3}$$

According to Pontryagin's minimum principle, [74], minimization of the cost J requires the scalar Hamiltonian function H to be minimized for each time instant $t \in [0, t_f]$, where t_f is the "final" time instant, when $\dot{Y} = 0$ and thus $Y = Y_{\max}$. This is given by:

$$H(\lambda(t), \mathbf{x}(t), \tilde{\mathbf{u}}(t)) = \lambda^T(t) \cdot \mathbf{f}(\mathbf{x}(t), \tilde{\mathbf{u}}(t))\tag{5.4}$$

Here $\lambda = [\lambda_1, \dots, \lambda_6]^T$, is the time-varying Lagrange multiplier vector adjoined to the constraints on the state equations; its elements are the *co-states* of the system and reflect the gradient of dynamic cost with respect to each state. In the absence of constraints, the minimum H is obtained by solving for \mathbf{u} in Eq.5.5:

$$\left(\frac{\partial H}{\partial \tilde{\mathbf{u}}}\right)^* = \mathbf{0}\tag{5.5}$$

The co-states are determined via the necessary condition Eq.5.6, with the boundary conditions Eq.5.7 for free-time optimal control problem:

$$\dot{\lambda} = -\left(\frac{\partial H}{\partial \mathbf{x}}\right)^T = -\left(\lambda^T \cdot \frac{\partial \mathbf{f}}{\partial \mathbf{x}}\right)^T = -\left(\frac{\partial \mathbf{f}}{\partial \mathbf{x}}\right)^T \lambda\tag{5.6}$$

$$\begin{aligned}
 \lambda_f &= \lambda(t_f) = \left(\frac{\partial J}{\partial \mathbf{x}} \right)_{t_f} = \left[\frac{\partial J}{\partial x_1}, \dots, \frac{\partial J}{\partial x_6} \right]_{t_f}^T \\
 &= [0, 0, Y_f, 0, 0, 0]^T
 \end{aligned} \tag{5.7}$$

Here, for clarity, we omit functional dependencies for H , λ , \mathbf{x} and $\tilde{\mathbf{u}}$.

We see that the boundary conditions of λ at time t_f are unknown due to the unknown t_f and Y_f . The state equations Eq.5.2 and co-state equations Eq.5.6 together form an extended state-space model: at time $t_0 = 0$, states \mathbf{x}_0 are known PI initial states while the co-state vector λ_0 is unknown; at time t_f , we only know $x_4(t_f) = \dot{Y}(t_f) = 0$. Hence, this optimal control problem is in the form of a **two-point boundary value problem** (2pt-BVP), i.e. the ordinary differential equations are required to satisfy boundary conditions at more than one value of the independent variable [75].

From Eq.5.4:

$$\begin{aligned}
 H &= H_0 + H_1 \\
 H_0 &= \lambda^T(t) \cdot \mathbf{f}_0(\mathbf{x}(t)), \quad H_1 = \lambda^T(t) \cdot B \cdot \tilde{\mathbf{u}}(t)
 \end{aligned} \tag{5.8}$$

Thus, the part of Hamiltonian directly influenced by $\tilde{\mathbf{u}}$ is H_1 :

$$H_1 = \lambda_2 \tilde{u}_1 + \lambda_4 \tilde{u}_2 + \lambda_6 \tilde{u}_3 \tag{5.9}$$

Since $\tilde{\mathbf{u}}$ appears linearly in the transformed state equations, $\tilde{\mathbf{u}}$ disappears after differentiation in Eq.5.5. This implies that the optimal control is fully determined by the active force and moment *constraints* of the system:

$$\min(H) \Leftrightarrow \min_{\tilde{\mathbf{u}}(t)} (\lambda^T(t) \tilde{\mathbf{u}}(t)) \tag{5.10}$$

The linear form of H_1 lends itself to a simple geometrical interpretation, see Figure 5.1. The blue shaded region U represents the bounded set of forces and moment (expressed as F_{xg}^{act}/m , F_{yg}^{act}/m and M_z^{act}/I_{zz}) available as the brake forces at the brake disks F_{wi} are varied. This representation was used previously in the analysis of actuator apportionment developed in [88]. In Figure 5.1, surfaces of constant H exist as planes in the 3D control space, and therefore the minimum value is achieved on the boundary of the "cloud" of available controls. In the figure, $\tilde{u}_1 = F_{xg}^{act}/m$ is suppressed, so the (blue) shaded area is the projection of the 3D cloud onto the F_{yg}^{act} - M_z^{act} plane, and the planes of constant H appear as a family of lines. As will be seen, the cloud is mostly convex, and the point of minimum H is almost always unique; here the point of tangency is indicated as a (red) dot. This position depends only on the direction of the normal vector to the planes, i.e. by the ratios between the three co-states, which further determine the balance between the global forces and moments. It should be noted: Hamiltonian

minimization makes full use of the nonlinear tyre forces, and the linearized equations are only used to compute the co-states ratio; this limited use of the linearized model is thought to explain the high degree of correlation to the results seen in the nonlinear open-loop optimizations [71, 94]. The minimum Hamiltonian is thus achieved by:

$$H_1^* = \min_{F_{xwi}} \sum_{i=1}^4 \left(\lambda_2 \cdot \frac{F_{xgi}^{act}}{m} + \lambda_4 \cdot \frac{F_{ygi}^{act}}{m} + \lambda_6 \cdot \frac{M_{zi}^{act}}{I_{zz}} \right) \quad (5.11)$$

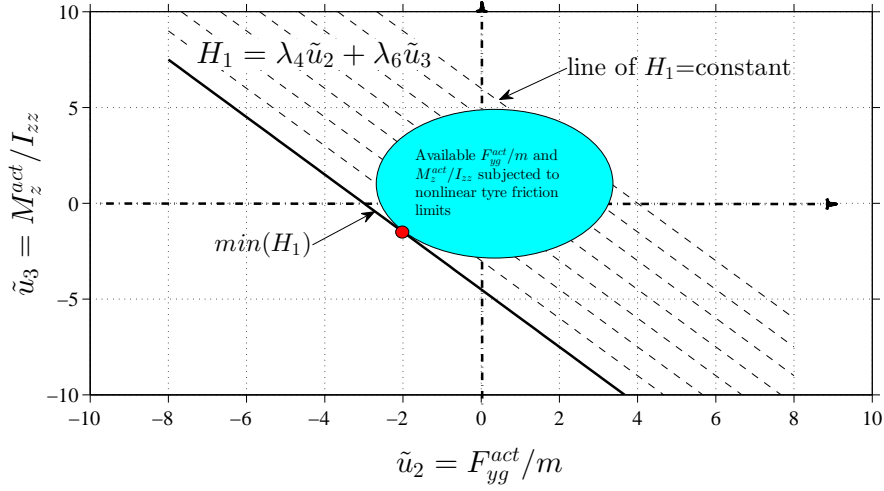


Figure 5.1: Hamiltonian Minimization Strategy ($\tilde{u}_1 = F_{xg}^{act}/m$ axis is suppressed for clarity). The shaded (blue) area represents the attainable F_{xg}^{act}/m , F_{yg}^{act}/m and M_z^{act}/I_{zz} subjected to nonlinear tyre force limits. The small (red) circle shows the optimal choice.

Hence, linearity in the state equations with respect to controls allows for considerable simplification in determining the optimal global forces and moments. Furthermore, it permits simplification of the H minimization, so that it can be cascaded to the individual wheel level (i.e. force allocation to brake force actuators), provided the difference of load transfer with different F_{xwi} is negligible. In this case the Hamiltonian of each wheel H_{1i} may be assumed to be independent of the applied braking forces at other wheels:

$$\frac{\partial H_{1i}}{\partial F_{xwj}} \approx 0, (i \neq j) \quad (5.12)$$

Hereby, the minimum H_i is achieved via proper choice of braking forces F_{xwi} and thus $\tilde{\mathbf{u}}$ may be found by performing minimization locally at each individual wheel i :

$$H_{1i}^* = \min_{F_{xwi}} \left(\lambda_2 \cdot \frac{F_{xgi}^{act}}{m} + \lambda_4 \cdot \frac{F_{ygi}^{act}}{m} + \lambda_6 \cdot \frac{M_{zi}^{act}}{I_{zz}} \right), \quad (5.13)$$

for $i = 1, \dots, 4$.

The resulting optimal choice for F_{xwi} requires only knowledge of the local nonlinear tyre force model, based on the instantaneous vertical tyre load. The validity of the cascading process including the approximation contained in Eq.5.12, and its influence on the optimality is discussed in Paper C.

Another approximation in the implementation of nonlinear optimal control is the implicit assumption that control constraints are independent of system states [74]. While individual brake forces at the wheels may be assumed to have fixed limits, the available forces and moments $\tilde{\mathbf{u}}$ depend on vehicle slip angle and yaw rate. However, we shall see in the examples below that, provided PI kinematics are not too extreme, the region of available forces and moments (as in Figure 5.1) is insensitive to the choice of applied controls and the optimality conditions remain valid. In the following section, a candidate approach to estimate the co-states is proposed, so that the complexity of the 2pt-BVP is reduced and real-time implementation is potentially feasible.

5.2.2 Candidate solutions to the BVP

Here we make use of a simple linear bicycle model [62] to approximate the solution of co-state differential equation and provide a candidate solution for the 2pt-BVP above. Firstly the six-state model above is reduced to four states: $\mathbf{x} = [Y, \dot{Y}, \psi, \dot{\psi}]^T$, and so does the co-states: $\lambda = [\lambda_1, \lambda_2, \lambda_3, \lambda_4]^T$. This is based on the observation that X -dynamics have little effect on the tyre side slip angles and thus little effect on the forces and moments influencing lateral dynamics. Since the control objective does not depend explicitly on X , with this assumption the Y and ψ dynamics are fully decoupled from that of X . At the same time the number of vehicle-level controls $\tilde{\mathbf{u}}$ is reduced to two: $\tilde{\mathbf{u}} = [F_{yg}^{act}/m, M_z^{act}/I_{zz}]^T$. Correspondingly the dimensions of vector λ , matrix B and C are also reduced.

The state-space model in Eq.5.2 is simplified in Eq.5.14 using the bicycle model:

$$\begin{aligned} \dot{\mathbf{x}} &= A \cdot \mathbf{x} + B \cdot \tilde{\mathbf{u}} \\ y &= C \cdot \mathbf{x} \end{aligned} \quad (5.14)$$

where:

$$A = \begin{bmatrix} 0 & 1 & 0 & 0 \\ 0 & p_{\dot{Y}_1} & p_{\psi_1} & p_{\dot{\psi}_1} \\ 0 & 0 & 0 & 1 \\ 0 & p_{\dot{Y}_2} & p_{\psi_2} & p_{\dot{\psi}_2} \end{bmatrix}, \quad B = \begin{bmatrix} 0 & 0 \\ 1 & 0 \\ 0 & 0 \\ 0 & 1 \end{bmatrix}, \quad C = [1 \quad 0 \quad 0 \quad 0].$$

The model is made linear by assuming small yaw angles $\psi(t)$ and constant longitudinal velocity v_x , and uses underlying linear tyre characteristics. We assume an average cornering stiffness defined in the range of sustained tyre side slip angles. The model in Eq.5.14 is subjected to the above mentioned control constraints on $\tilde{\mathbf{u}}$, since friction limits are respected at each individual wheel. The elements of the A matrix are constant parameters here and depend on the specific vehicle parameters chosen. In closed-loop real-time implementation, A can then be updated at each time instant according to the instantaneous v_x . See Appendix C of Paper C for the full form of A matrix. After linearization, the structure of the Hamiltonian is as follows:

$$\begin{aligned} H &= \lambda^T \cdot (A\mathbf{x} + B\tilde{\mathbf{u}}) \\ &= \lambda_1 x_2 + \lambda_2 (p_{\dot{Y}_1} x_2 + p_{\psi_1} x_3 + p_{\dot{\psi}_1} x_4) + \lambda_3 x_4 + \\ &\quad + \lambda_4 (p_{\dot{Y}_2} x_2 + p_{\psi_2} x_3 + p_{\dot{\psi}_2} x_4) + \lambda_2 \tilde{u}_1 + \lambda_4 \tilde{u}_2 \end{aligned} \quad (5.15)$$

It is seen that the part influenced by the control inputs is $H_1 = \lambda_2 \tilde{u}_1 + \lambda_4 \tilde{u}_2$, and is reduced from that in Eq.5.9.

It is then straightforward to apply the linearized state matrix A for co-state estimation. The co-state equations Eq.5.6 become linear with constant coefficients, and an explicit form of the solution exists:

$$\dot{\lambda} = -(\lambda^T A)^T = -A^T \lambda \quad (5.16)$$

$$\lambda(t) = e^{-A^T(t-t_f)} \cdot \lambda(t_f) \quad (5.17)$$

where $\lambda_f = \lambda(t_f) = [Y_f, 0, 0, 0]^T$. The solution depends on two parameters, Y_f and t_f , but since the optimal control only depends on the co-state ratios (recall Figure 5.1) this leaves just one unknown parameter, t_f to be determined in order to find the candidate optimal control. In Paper C, the question of t_f estimation is tackled in the closed-loop form of the controller.

5.2.3 Closed-loop controller

A closed-loop form of the QLOC control system is shown in the block diagram, Figure 5.2. The figure summarizes the candidate approach of solving the 2pt-BVP discussed above. Knowing the vehicle states from measurements and state observers on-board, t_f is estimated and fed into the λ calculator.

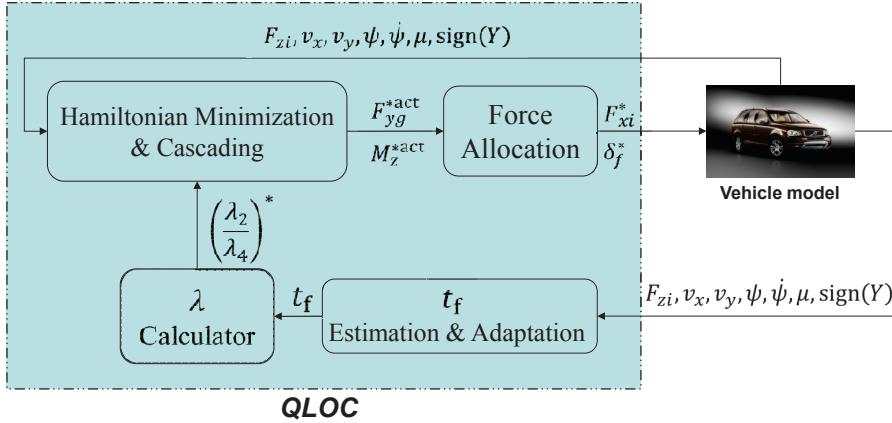


Figure 5.2: Block diagram of the closed-loop controlled system.

In the closed-loop form, the *co-states calculation* and *Hamiltonian minimization* are carried out at each time step during the control, and even though a complete control sequence is evaluated (for t_f estimation) it is only the initial control values that are applied; in this aspect the method has similarities to the Model Predictive Control (MPC) method mentioned above; extensive studies about the stability analysis and computational performance of MPC can be found in [95–98]. It is worth noting some differences between these two approaches: (a) MPC typically assumes a prescribed fixed horizon time for control, whereas QLOC estimates and updates this prediction horizon continuously. (b) MPC typically linearizes the plant dynamic model and calculates the minimum of a quadratic cost function, which may limit the overall accuracy; QLOC linearizes only that part of the dynamic model which is used for the calculation of co-state ratios, whereas the full nonlinear tyre forces are used for Hamiltonian minimization. (c) Regarding nonlinear MPC, the computation is demanding and optimization convergence is hard to guarantee; here, QLOC only executes plant simulation to estimate a single parameter, t_f , but not to compute the control signals. The fact that QLOC is formulated in continuous time also appears to be a distinct advantage, as discretization errors can be avoided.

In Paper G, the controller above is further developed for regulating longitudinal and lateral deviations simultaneously; thus for instance both lateral deviation and terminal speed may be simultaneously controlled. Although cost in integral form, as J_1 with $f_1 = 1$ introduced in the previous chapter, is favorable for problem definition and smooth numerical optimization, it is less feasible to provide explicit solution for closed-loop optimal controller design. Rather, similar to the cost function Y_{\max} used above, a simple function

describing the cost at final time is proposed; this penalizes the final velocities instead of displacements, and turns out to be capable of approximating results from J_1 optimization, and crucially, is also amenable to real-time solution of the two-point boundary value problem posed by optimal control theory; see more about the problem formulation in Section II of Paper G. Hereby, all the six states including the longitudinal dynamics of vehicle planar motion are considered in the control system and thus the control input vector is extended back to $\tilde{\mathbf{u}} = [F_{xg}^{\text{act}}/m, F_{yg}^{\text{act}}/m, M_z^{\text{act}}/I_{zz}]^T$. There a particle motion and linear bicycle model are used to calculate the reference control inputs $\mathbf{u}^{\text{ref}}(t)$ for a pre-simulation. The vehicle states acquired via the pre-simulation are the reference states, around which the nonlinear vehicle system equations are linearized. In the same way as before, *the linearized model is only used to compute the co-states ratios that will provide the optimal trade-off between the global forces and moments*. Paper G shows that the extended controller provides satisfactory control performance compared to the independent open-loop numerical optimization.

5.3 Under-determination in control allocation at tyre friction limits

The comparisons between open-loop numerical optimizations and closed-loop optimal controller have shown that different types of vehicle motions can result in approximately the same value of the prescribed cost function, see example cases in Paper C, Paper D and Paper G. This can be possibly explained by the under-determination of optimal vehicle level forces and moments given the predefined costs and constraints. This under-determination can provide opportunity for enhanced *control authority* and reduced *control effort* via appropriate adjustments to the *control allocation*. With respect to control authority, it indicates some freedom to reduce a secondary cost without compromising the optimum of the primary cost function that is most important for mitigating the subsequent collisions; with respect to control effort, different vehicle response requires different actuator control modes so that the minimum and smoothest control efforts can be applied to achieve the same optimum. Since the degree of this under-determination also depends on the availability of vehicle level forces and moments which are produced by different actuator configurations, the next level of under-determination, i.e. control allocation from vehicle level to individual wheel level, is of great interest.

On one hand, just three vehicle response variables are controlled (F_{xg} , F_{yg} and M_z) with five actuators (4 individual wheel brakes and 1 front axle

steer) and therefore some redundancy is to be expected. From this perspective it is possible that many actuator controls can map to the same vehicle level force and moment. On the other hand, as illustrated in Figure 5.1, the optimal control sits on the boundary of the domain (cloud) of available global forces and moments; the reason is expected to be: tyres are usually at friction limits after external impacts, and each actuator is operating at own bandwidth and amplitude limit; in that case uniqueness of actuator controls is more likely. In an attempt to improve understanding of uniqueness, in Paper E, a related question was investigated, namely the sensitivity of vehicle response to the individual actuator controls. This study used the optimal control sequences obtained by numerical optimizations, given the cost function in Eq. 5.18, with two sets of parameters: (1) $a = 0, b = 1$; (2) $a = 1, b = 1$.

$$J_1 = \int_0^{t_f} (a \cdot X^2 + b \cdot Y^2) \cdot dt \quad (5.18)$$

where $\dot{X}(t_f) = 0$.

To test the uniqueness and sensitivity to actuator controls, all points $(F_{xg}(i), F_{yg}(i), M_z(i))$ in the cloud within a small neighborhood of the optimal choice (red dot in Figure 5.1) $(F_{xg}^*, F_{yg}^*, M_z^*)$, are retrieved and the corresponding actuator control values are traced for each point. The method of cloud construction is useful here: a ‘‘brute force’’ allocation approach was used, varying the braking forces and steer angles on a discretized grid, and aggregating to the corresponding vehicle level forces and moments. At this point, the rate limits of steer and brake actuators are not considered, i.e. it is assumed that actuation requests can be achieved instantly within the bounds of minimum and maximum.

The neighborhood is defined by limiting the relative change from optimal control values:

$$\left(\frac{F_{xg}(i) - F_{xg}^*}{F_{xg}^*}\right)^2 + \left(\frac{F_{yg}(i) - F_{yg}^*}{F_{yg}^*}\right)^2 + \left(\frac{M_z(i) - M_z^*}{M_z^*}\right)^2 < Q^2 \quad (5.19)$$

The tolerance Q is constrained to a very low value $Q = 2\%$.

The alternative steering and braking actuation of cost function (1), i.e. $a = 0, b = 1$ in J_1 , are shown below in Figure 5.3 and Figure 5.4. It is seen that quite different actuator modes can provide almost the same global forces and moments, in which case the mapping between actuator controls and vehicle level forces and moments is ill-conditioned. Further studies in Paper E showed that without X dimension in the cost function, a wide range of actuator modes will lead to relatively more different F_{xg} than different F_{yg} and M_z . This implies that additional constraints might be

imposed without compromising the post impact path lateral deviation, e.g. it is possible that vehicle speed can be reduced at mean time, given that the change of F_{xg} at current time step will not largely affect the availability of F_{yg} and M_z in future time steps.

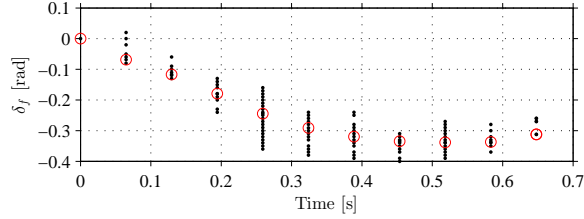


Figure 5.3: Steering angles (black dots) which generate global forces and moments closely adjacent to the optimal choice. Red circle denotes the optimal choice. $a = 0, b = 1$ in J_1 .

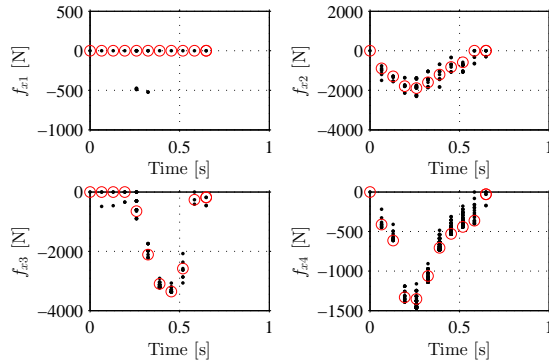


Figure 5.4: Braking forces (black dots) which generate global forces and moments closely adjacent to the optimal choice. Red circle denotes the optimal choice. $a = 0, b = 1$ in J_1 .

On the other hand, when we explicitly add X dimension in the cost function, e.g. $a = 1, b = 1$ in J_1 , the redundancy of actuators modes is found to be reduced significantly, see Figure 5.5 and Figure 5.6. That is to say, the vehicle response becomes quite sensitive to the individual actuator controls if F_{xg} is also *specifically* requested, together with specified F_{yg} and M_z , i.e. the mapping between actuator controls and vehicle level forces and moments are better-conditioned. It is also interesting to note that two different vehicle responses can result in the same cost, as shown in

5.3. UNDER-DETERMINATION IN CONTROL ALLOCATION AT TYRE FRICTION LIMITS

the Figure 4 in Paper G. As mentioned above, this is due to the under-determination of vehicle level forces and moments, and it is expected that if the dimension in the cost function is further increased, e.g. yaw angle is also penalized, the optimal controls and thus the vehicle motion will be more unique.

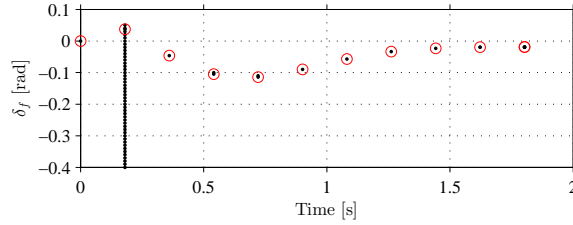


Figure 5.5: Steering angles (black dots) which generate global forces and moments closely adjacent to the optimal choice. Red circle denotes the optimal choice. $a = 1, b = 1$ in J_1 .

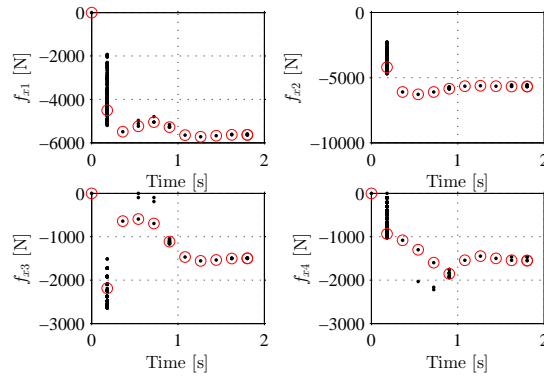


Figure 5.6: Braking forces (black dots) which generate global forces and moments closely adjacent to the optimal choice. Red circle denotes the optimal choice. $a = 1, b = 1$ in J_1 .

It is worth noting that ill-conditioning mentioned above is not necessarily a practical issue, since it may disappear when bandwidth limits imply control actions are fundamentally continuous; one cannot simply jump between equivalent but widely separated actuator control modes during closed-loop control. That is to say, ill-conditioning may disappear when actuator limits are imposed; this may be achieved in the optimization, by penalizing any rapid changes at the actuator level, or simply respecting the actuator bandwidth limits. To test this, the sensitivity analysis was repeated but

now imposing rate limits based on actuator bandwidths assumed in the optimization model. In this case it was indeed found that the multiplicity of available solutions disappears, thereby it shows the bandwidth affects actuator freedom to a large extent, and ill-conditioning is not likely to give any genuine concern for future implementation of the closed-loop control in real time.

Chapter 6

Function Design and Verification in Experiments

6.1 Function design

The function design of the PIC system is closely related to the identification of PIC-relevant cars during the accident research presented in Chapter 3. Based on the knowledge about typical post impact vehicle dynamics and accident scenarios, the functional structure of the PIC system is proposed as a *discrete state diagram*, see Figure 6.1 below. Here the name *state* refers to a *discrete event* in each execution cycle of an algorithm; this is different to the *continuous* states usually used in the contexts of dynamical system modelling. The diagram shows the conditions to activate next state and to deactivate current state in the PIC function at the different states during a post impact accident scenario.

To prevent any false function activation due to sensor malfunction, signal noises and other irrelevant disturbance events such as hitting a rock under vehicle body, correct and timely impact detection and characterization are critical for the satisfactory performance of PIC function. This requirement is certainly similar to the triggering of airbag systems in the vehicles nowadays. As known, for one type of passenger vehicle, the airbag triggering threshold not only depends on the speed change (Δv), but also the vehicle deceleration, vehicle rotational velocities, impact force magnitude, position and direction etc.; different airbag system manufacturers have different algorithms to blend these factors for the decision making about airbag deployment. The general applicable values of the airbag triggering thresholds can be $\Delta v \geq 20$ km/h for frontal impacts, and $\Delta v \geq 15$ km/h for side or rear impacts. Previous analysis of the GIDAS accident database has shown that if these thresholds can be lowered to $\Delta v \geq 5$ km/h, the number of PIC-relevant cars can be approximately doubled. This indicates

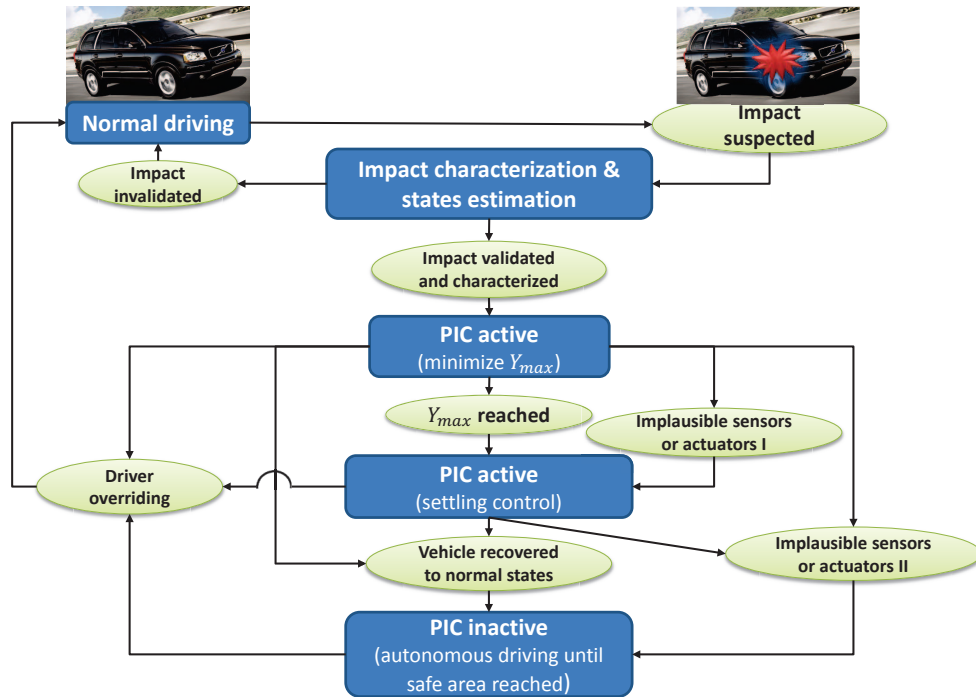


Figure 6.1: Discrete state diagram of the PIC function. Blue boxes: discrete states, green circles: conditions for state transitions.

that the number of cars that will eventually gain safety benefits from the PIC system can be greatly increased as well. It is expected that this lowered Δv threshold can possibly be measured by the advanced impact force or acceleration sensors. As known, the brake and steer actuators typically have some time delays before any torques being applied, hence in order to save actuation time, the PIC function can be already activated once the Δv threshold is reached (this state transition is omitted from the structure shown in Figure 6.1). Unlike the deployment of airbag, the PIC activation can be canceled during the delay time of the actuators. This possibility further motivates the selection of lowered Δv threshold, which was applied for filtering the accident cases studied in [67]. The real-world impact cases used in the experiments for function verification all have Δv larger than 5 km/h, however the impacts are sufficiently light that the airbag system nowadays would unlikely be triggered.

Once the changes of velocities, e.g Δv above, exceed the corresponding thresholds, a PIC-relevant impact event can be suspected. To validate and characterize the impact, several consecutive samples of the vehicle states measurements and estimation should be accessed and analyzed, typically

before the end of the impact. This algorithm can be integrated with the crash sensors in the airbag ECU. Collision mechanics models based on the momentum equilibrium are usually used to estimate the impulse characteristics and thus to predict the vehicle states during the impact [49]. These predicted values of certain vehicle states can be compared to the measurements from gyros and the estimations from observers. The agreement between these two signal sources will then issue a checksum as secured communication message after which the PIC function is activated. However, if a disagreement is detected, the suspected impact is invalidated so that the PIC function stays inactive while *normal driving* continues.

Based on the traffic situation and road layout where the initial impact occurs, the direction of maximum risk for a secondary collision of the PIC-relevant car can be determined in real-time, as discussed in Section 4.4. In Figure 6.1, the structure is shown for the PIC function proposed in the previous work where it is critical to *minimize the maximum lateral deviation* immediately after the initial impact. The assumption here in the real-world scenario is that the road is straight and sufficiently wide in order to avoid the subsequent impact given the Y_{\max} is effectively minimized.

As mentioned before, it is possible that at the point of Y_{\max} , vehicle dynamical states are still outside the normal operational range of conventional active chassis control systems, and possibly the capability of a normal driver as well. Thereby, in this situation, the second phase of the controller (settling control, as shown in Figure 5.2) should be activated so as to help settle down the vehicle states while tracking a reasonable path profile in the road coordinates.

The PIC function is considered as a “safety net” which should only be activated in impact-related emergency situations. Hence, with the vehicle having recovered to normal motions, the PIC function should be disengaged and hand the control authority back to the autonomous driving systems until the vehicle is successfully directed to a safe area, e.g. by the side of the road. These autonomous functions can include the AEB system together with an auto-hold electronic parking brake system which will keep the car stationary within the safe area. It is also possible that the driver stays or has recovered to normal mental and physical states so that he/she can be capable of taking full control of the vehicle motion again. This concludes a complete loop of the activation and deactivation of the PIC function.

At a set of extraordinary conditions, control requests from the PIC function can be aborted for different reasons. As shown by the “Driver overriding” block in Figure 6.1, for instance, if driver has deliberately moved the right foot from brake pedal to gas pedal and afterwards apply a strong positive acceleration, it indicates the driver is alert and intended to control

the vehicle by him/herself. It is also possible that prior to the accomplishment of the prescribed control target, e.g. to reach Y_{\max} , the vehicle may have already recovered to the normal states so that certain autonomous driving systems or the driver can take the control of the vehicle directly at this point. At different discrete states of the post impact vehicle control, the requirements on the amount and quality of sensors and actuators can differ, e.g. settling control may not require the road friction and vertical loads which are estimated from the measured accelerations and velocities. Hence, if some implausible signals are detected, the control task can be transitioned to the next state which would work efficiently with the signals still available.

6.2 Verification methods for driver interaction

As mentioned before, after the impacts which are of high severity, the driver can be disturbed to an extent that he or she experiences panic and hence steps out of the control loop. In this situation, without inputs from driver interaction, vehicle simulation models and autonomous vehicles can be directly used for function verification. On the other hand, as seen from the results of accident analysis in Chapter 3, a number of PIC-relevant vehicles were exposed to relatively mild initial impacts that the secondary events occurred probably due to improper reactions of the drivers. Hence, in order to clarify how drivers react during and after impacts, high-fidelity and repeatable tests including drivers should be conducted. The challenge here is, without harming the test driver, to excite and place the test vehicle to various typical post impact motions. In the following, the capabilities of several approaches to achieve such excitations are discussed. The methods are evaluated using a 4-DOF (longitudinal, lateral, yaw and roll) two-track passenger vehicle model that incorporates collision mechanics in terms of friction and restitution coefficients. The results provide critical hints to design a verification method which can be applied in the future PIC function development.

6.2.1 Precision immobilization technique

Precision Immobilization Technique (PIT) is a deliberate manoeuvre that a pursuing car forces the pursued one to abruptly turn sideways to the direction of travel, causing the driver to lose control and stop [99]. This is a method mostly used to end a *car chase* more safely and thus it appears as a judicious method for police cars to terminate a hazardous vehicle pursuit

6.2. VERIFICATION METHODS FOR DRIVER INTERACTION

with the criminals. The Figure 6.2 below shows the procedure of a typical PIT manoeuvre.

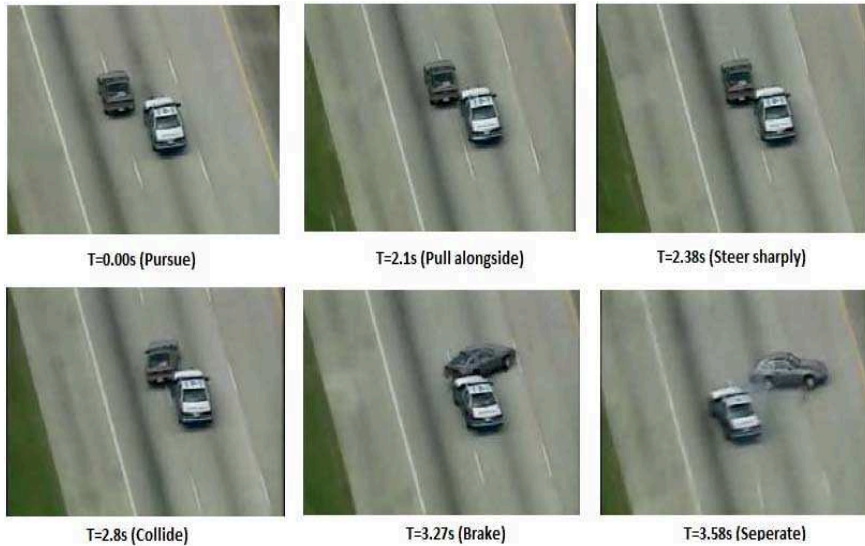


Figure 6.2: A real PIT manoeuvre record [29].

Here this technique was studied via simulations, and several issues were particularly considered for driver safety and sufficiently low damage to the PIC test car.

- It is assumed that steel bumper is well covered over the body of host car at the height of intended collision. The bumper which has relatively high stiffness can prevent noticeable deformation of the test car. Instead, soft crush zones could be installed to the bullet car. No detailed structural mechanics were directly modeled for accounting the energy loss, instead a coefficient of restitution was assumed: 0.2.
- The impact positions were mainly chosen at rear end of the host car, complemented with rather light ones at the far side of the driver.
- According to the injury criteria, during the impact, the maximum accelerations for rear-end crashes and side crashes were limited to 20 m/s^2 and 8 m/s^2 respectively. Impact duration was chosen according to an average value for most real accidents: 0.2 s. In order to

satisfy these limitations, the impulse magnitude was less than 6500 Ns for rear-end crashes and less than 2500 Ns for side ones.

To assess the destabilization capabilities using PIT manoeuvres, the host vehicle dynamics was simulated using a set of initial speeds ($v_x \in [5, 40]$ km/h) and impact angles ($\theta_{\text{imp}} \in [-90, 90]^\circ$). Figure 6.3 below shows the attainable region of post impact yaw rates and side slip angles; the axis for post impact speeds is suppressed for the clarity of the illustration.

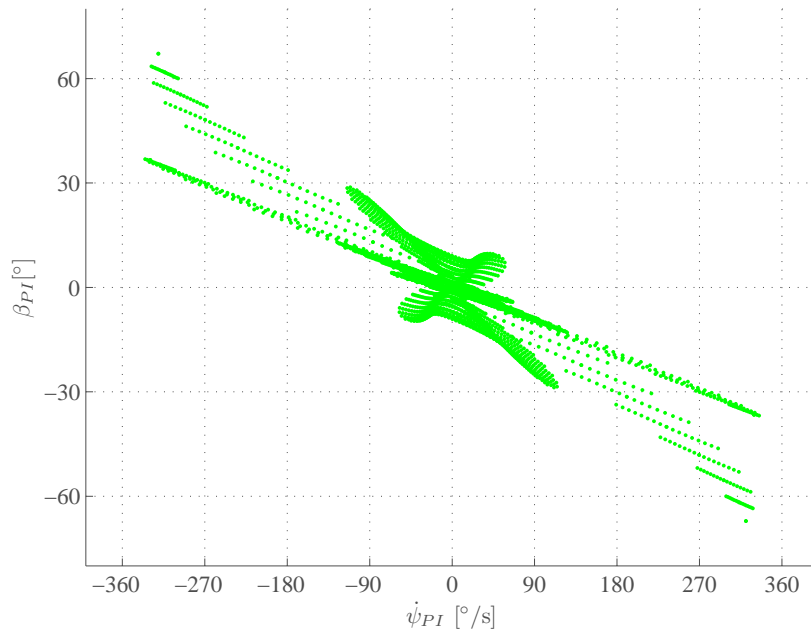


Figure 6.3: The capability region of *PIT manoeuvres* [70].

It can be seen that most of the scattered dots reside in the 2nd and 4th quadrants due to the limitations of impact positions and magnitudes mentioned above. This indicates that PIT manoeuvres can generate relatively high side slips and yaw rates of *opposite* signs, while very low magnitude with the *same* sign can be achieved. Furthermore, the ratio of these two quantities are constrained around a certain value, as shown in Figure 6.3.

6.2.2 Destabilization using built-in actuators

This method is essentially designed to *control* the vehicle actuators in an opposite way to the stability control systems on-board. The three common built-in actuators are propulsion torque at the driven axles, brake torques at each wheel and assist steering torque at front axle. In the present study,

front-axle steer and individual-wheel brake actuators are assumed available in the test vehicle.

It was found that the traditional test manoeuvres such as *sine with dwell* designed for evaluating ESC systems are incapable to generate as similar and high disturbances as an impact [67]. Inspired by the drifting techniques used by rally drivers, the destabilization concept is developed: saturate the lateral grip of rear tyres in a cornering manoeuvre, and abruptly apply hard braking on rear wheels until the steering angle has returned to zero.

Here different steering and braking ramp-up rates and start-end time instants were tested on wet and dry road conditions, with various vehicle entering speeds before the destabilization. Figure 6.4 below shows the capability region of this method. In brief, using the built-in actuators, the vehicle can be placed at the yaw rate ($\dot{\psi}_{PI} \in [-100, 100]$ °/s) and the side slips ($\beta_{PI} \in [-90, 90]$ °) which have the *opposite* signs. It can be seen that only the amplitude of post impact yaw rate but not the side slip angle is limited. This pattern is similar to the PIT manoeuvre, while with wider coverage of the side slip angles and narrower coverage of the yaw rates.

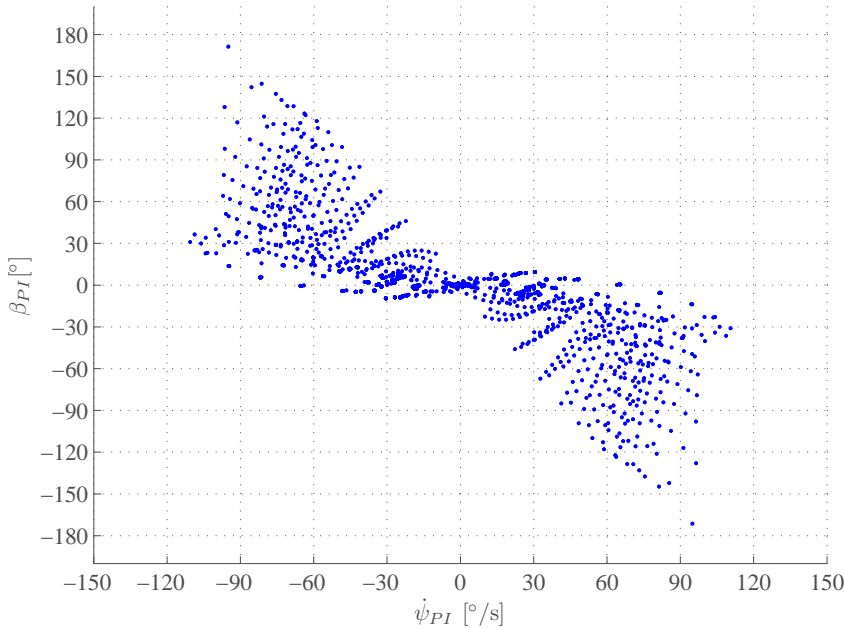


Figure 6.4: The capability region of *built-in actuators* [70].

6.2.3 Kick plate

Kick plate is a hydraulic facility which actively engages various electronic systems. The plate can generate a “kick” laterally when the vehicle rear wheels pass over [100]. In front of the kick plate, there is normally a *performance surface area* which has low friction, so as to test the driver’s ability of controlling an unstable vehicle. It is also used to demonstrate the latest automotive safety technology. The Figure 6.6 illustrates the test environment using a kick plate. It proves to have high repeatability and safety incorporated with the complete test track; while the cost and construction complexity are found to relatively high as well.



Figure 6.5: Destabilize a car using kick plate (low friction surface designed after the kick) [101].

The kick force comes from the tyre lateral forces which are certainly limited by the plate-tyre friction coefficient. Hence the generated lateral acceleration is limited to approximately $1g$. The magnitude of the disturbance is affected by the plate size, plate lateral stroke, and the plate lateral speed which depends on the stored energy of hydraulic pumps. Based on the product specification by [101], simulation results show that the limiting factor is not the pump power but the plate-tyre friction. The possibilities to increase the plate size especially its depth, as well as lengthening the stroke

was investigated.

According to the characteristics of the kick plate equipment summarized above, five set-ups of “kick” were emulated with a set of entering speeds between 9 m/s and 40 m/s [70]. As expected, kicking the rear tyres on long-stroke plate generates the highest side slip angle, up to approx. 14 °; having two short-stroke plates kicking the front and rear axles respectively in the opposite direction gives the best yaw disturbance, up to approx. 80 °/s. Figure 6.6 shows the capability region of kick plate with the aforementioned five set-ups. The reachable “post-kick” states appear to be rather low, compared to the *PIT manoeuvres* and the *built-in actuators* approaches.

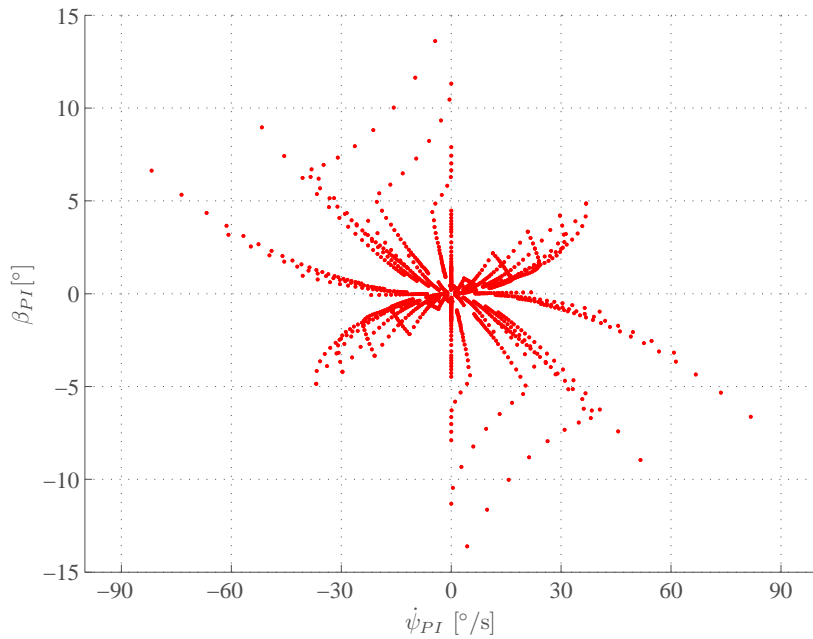


Figure 6.6: The capability region of *kick plate* [70].

6.2.4 Motion-based driving simulator

Driving simulator is a quite different candidate compared to the other approaches discussed above. In the simulator environment, the main goal is not to replay precisely the intended motion but to make the driver believe that he or she is experiencing this motion. Here, for the verification of *post impact* control system, we consider the most critical motion that should be sensed by the driver is the one immediately *after* impact. Thus, the accelerations *during* the impact, which may impose high human injury risk, can be scaled down. For emulating the post impact motions, the visual and audio

systems can provide any “velocities” on the graphic interface (screen) and the corresponding sounds into the driver’s ears. However, these “visualized velocities” can not be so high that the driver perception mismatches with the actual cabin motion. This requires a decent collaboration between several sub-systems at different layers of the simulator architecture. Simulator experts at Swedish National Road and Transport Research Institute (VTI) have stated: a typical scaling factor in motion cueing is 0.7 which means the driver gets a feeling of being moved 1 m if the cabin moves 0.7 m. This value may be tuned with different ranges of the velocities and accelerations in various specific driving scenarios.

Figure 6.7 below shows the new simulator constructed at VTI (Göteborg). It consists of two parts: a XY-table providing large stroke linear motions in the longitudinal and lateral direction simultaneously and a hexapod providing 6-DOF motion within the stroke capability of the actuators [102].



Figure 6.7: Simulator IV at VTI (Göteborg) [102].

According to the simulator parameters provided by VTI, the *motion cueing* on yaw rate is estimated:

$$\dot{\psi}_{\text{SIM4}} = \frac{a_{n_{\text{cabin}}}}{v_{t_{\text{cabin}}}} \quad (6.1)$$

where $a_{n_{\text{cabin}}} \approx 6\text{m/s}^2$ is the limit of centripetal acceleration that can be generated, based on both the power of hydraulic system for the XY-table and hexapod and the injury criterion for human; $v_{t_{\text{cabin}}}$ approximates the simulated post impact speed.

Figure 6.8 shows the reachable yaw rates at different post impact speeds. As expected, in the simulator, the attainable region of post impact yaw

rates shrinks as the speed increases. The reachable side slip angle is within $[-90, 90]^\circ$ since purely lateral velocity can be generated by the XY-table alone, although the available time duration is limited by the table's excursion range (5 m in Y direction).

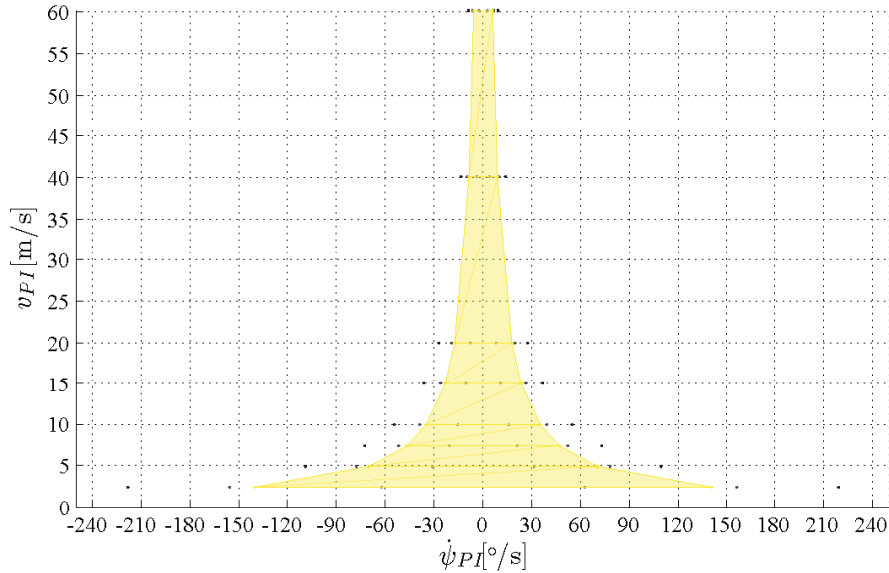


Figure 6.8: The capability region of the motion-based *driving simulator* at VTI (Göteborg) [70].

6.2.5 Summary of verification methods

The Figure 6.9 below shows the coverage capabilities of the four methods introduced above, in a 3-D space: PI speed, yaw rate and side slip angle. It was estimated that 60% of the 856 PIC-relevant cars can have the PI kinematics be reached by PIT manoeuvres, and the corresponding percentages for built-in actuators, kick plate and driving simulator (Simulator IV in VTI) are 50%, 20% and 40% [70].

Furthermore, 10 impact cases from the 14 *chromosome* groups identified via the previous accident analysis (see Paper A and Chapter 3) were evaluated in fine details using these four candidate methods. These example cases can represent 75% of the 856 cases. The 10 examples here also provide a test matrix in driving experiments with the PIC function. In brief, it was found that 5 cases can be achieved by PIT manoeuvres, and the corresponding numbers for built-in actuators, kick plate and VTI Simulator IV are respectively 5, 1 and 2. Nevertheless, the *effective* capability of the driving simulator will be higher if the motion cueing and visualization techniques can be properly designed. Regarding the other factors apart from the

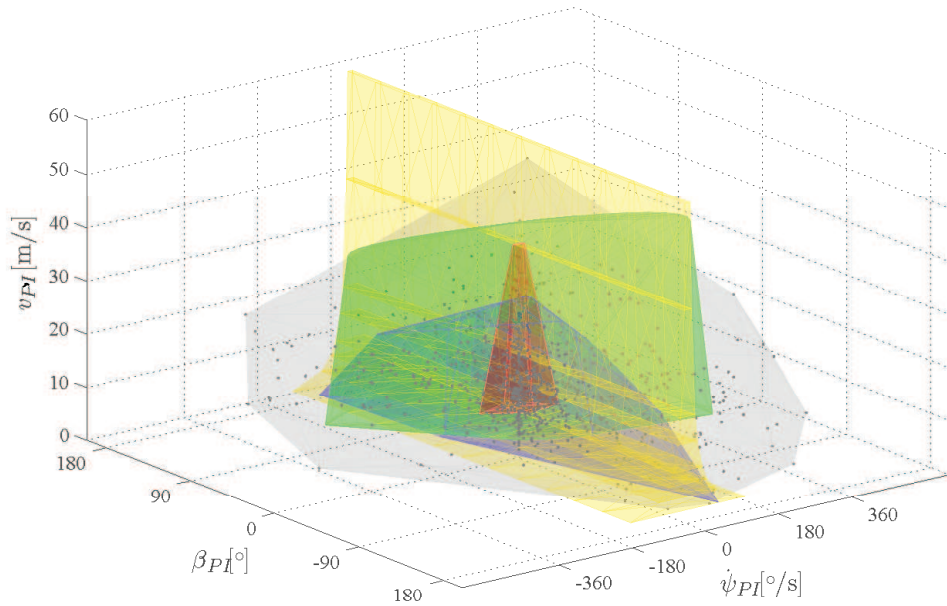


Figure 6.9: The capability region of *PIT manoeuvres* (green), *built-in actuators* (blue), *kick plate* (red) and *VTI Simulator IV* (yellow), covering post-impact kinematics of the PIC-relevant cars (grey) [70].

capability, e.g. accuracy, repeatability, driver safety, cost etc., the driving simulator method was ranked the best for conducting the experiments in a post impact scenario with driver interaction [70].

6.3 Verification in driving simulator

The function design proposed above was applied to the function verification experiments in a driving simulator environment. Initially the evaluation method is developed with the focus to capture different types of disturbances to the vehicle motions, rather than on the driver visual distraction prior to an initial impact. It is assumed that driver is not disturbed in any sense until the impact happens; nevertheless crash noise and accelerations associated with impacts are well emulated in the simulator environment.

As a first application of the method, a generic Post Impact Braking (PIB) which is similar to the SCM function ([20,21,30]) was developed and evaluated, together with a simple Anti-lock Brake System (ABS); four representative impact scenarios extracted from the GIDAS accident database were reproduced; the PIB function is evaluated by three types of driving styles, namely *normal*, *alert-skilled*, and *passive* drivers, assuming either the ABS is functioning or ABS becomes malfunctioned due to damaged sensors

after impact. The experiment was conducted in a motion-based car driving simulator at Chalmers University of Technology and preliminarily verified in the higher-fidelity driving simulator at the VTI Gothenburg office. For the verification of PIB, the function is deactivated once any of the following three conditions is satisfied:

Accelerator pedal overriding The driver overrides the function by pressing the accelerator pedal hard, i.e. 95% of full pedal displacement.

Brake pedal overriding The driver overrides the function by pressing the brake pedal hard, i.e. 95% of full pedal displacement.

Vehicle recovered to normal states The function is deactivated if the vehicle speed v_x is less than 0.01 m/s over a certain time period, i.e. for 1.5 s.

As shown in Table III of Paper H, on average, the sequence of *normal* driver actions after impacts is: steering, releasing the accelerator pedal and then braking. At some runs, steering and releasing accelerator pedal occurred simultaneously. Braking usually occurs much later than the first two actions. The reaction time of steering is around 0.5 s or less, which is considered as the reflex delay in the muscles of ordinary humans. It is understandable that longer time is needed to apply braking than steering, since the leg muscle has longer delay when moving foot from accelerator to braking pedal [60]. It was also interesting to note that the subject drivers all experienced surprise and panic, even after repeated exposures to the impacts. None of the drivers was aware of the PIB intervention even after the test. It would be worth measuring the level and pattern of surprise and panic via certain medical devices attached to the driver, so as to estimate the fidelity of the experiment in terms of driver reaction. For the *alert-skilled* drivers, they react relatively faster by steering compared to the *normal* drivers; and they deliberately hold the vehicle speed by not releasing the accelerator pedal immediately after impact.

The performance of PIB is quantified by comparing certain post impact states when the function is enabled and disabled. The results in Paper H show that, PIB helps the drivers to lower the risk and severity of secondary collisions with respect to reduced longitudinal and lateral displacements and road leaving speed; whereas it leads to higher risk for possible side collisions due to increased yaw angle; these influences seem to be more considerable when no ABS function is available. *Passive* drivers are found to gain more benefits than *alert-skilled* drivers since full-braking degrades the vehicle steerability and thus the lateral and yaw response.

In addition, the QLOC algorithm proposed in Chapter 5 was tested in the Chalmers simulator, and further tests are ongoing in the VTI simulator. Similar to the PIB function above, QLOC is deactivated if any of those three overriding conditions occurs. Here the actuator configuration using friction brakes at individual wheel and steer-by-wire at front axle is simulated. After Y_{\max} is reached, PIB (full-braking with ABS) is activated as the *settling control* part of the PIC function. In the Chalmers simulator, two homogeneous groups of *normal* drivers were exposed to the same impact scenario, while respectively having QLOC and PIB as the main part of PIC function prior to Y_{\max} . Preliminary results have shown that QLOC can be well computed and executed in the real-time test environment. Similar to the performance observed in the off-line computer simulations, QLOC could optimally control the Y_{\max} . Compared to the PIB function, QLOC further reduces the lateral deviation and yaw angle while imposing higher yaw rate and longitudinal speed at Y_{\max} . The time window for QLOC intervention is so short that no driver noticed the function during the tests; however some drivers exhibited confusion on their faces probably due to the loss of steering torque feedback during the QLOC intervention. The ongoing experiment in the VTI simulator has indicated that the immediate steering torque application on the steering wheel appears to be much faster than any driver reaction even if the driver is mentally prepared for the impact disturbance.

As indicated by the completed experiments, driver braking may have sufficiently long delay that motivates the autonomous brake intervention by PIC. However, driver steering could come so fast after the initial impact that the steer-by-wire configuration certainly deteriorated steering feel and thus may induce confusion for the driver. It is expected that an EPAS system should be properly designed in order to provide optimal wheel steer angle as well as credible and safe torque feedback at the steering wheel. The topic about steering arbitration between the driver and the PIC function request is recommended for the future implementation in driving simulator and real vehicle tests.

Chapter 7

Conclusions and Recommendations for Future Work

7.1 Conclusions

This research aims to make systematic progress towards solving a real-world traffic safety problem that has been threatening human lives: multiple-event accidents (MEAs) where the passenger vehicle is subjected to more than one event, and the severity of the entire accident is intensified by the subsequent events. The envisioned solution is to actively control the vehicle motions after a primary collision in MEAs, as a critical complement to any on-board injury prevention systems.

To provide a solid foundation in understanding the underlying causes of secondary collisions in MEAs, accident data were first studied so that the vehicle directional control problems after impacts were characterized, in terms of both the vehicle dynamics states and the accident scenarios. To resolve one dominating symptom of the problem, i.e. excessive path lateral deviation, the trajectory optimization techniques were adopted to identify the optimal path control strategy which was found to be distinctive compared to the conventional stability control functions. Thereafter, a closed-loop quasi-linear optimal path controller was proposed to provide an approximation to the optimal strategy found in open-loop numerical optimizations. The resultant balanced control between global lateral force and yaw moment was further allocated to the optimal individual wheel brake torque and front axle steer angle requests.

In real-world road traffic, the safe area for vehicle travelling can evolve continuously in time. Hence, an on-line estimation of the direction of maximum crash risk is important in order to effectively avoid or mitigate the

subsequent events in real-time. In this thesis, a general form of the cost function was proposed to consider the expected crash risk and severity, which can be estimated with the sensor signals in the vehicle and infrastructure. An example of this cost formulation was applied in the optimal path controller which limits both the longitudinal and lateral deviations from the point of initial impact.

Considering the uncertainties in driver and vehicle states estimation as well as in environment sensing, it can be demanding to achieve the exact solution of the optimal vehicle motion control after impacts. Nevertheless, the work in this thesis has shown that significant improvement in vehicle traffic safety can be achieved if the optimal control strategy can be realized using the available actuators on-board. Results from the simulations and the ongoing experiments in driving simulators suggest that, the safety benefits gained from optimal tyre force re-distribution can not be underestimated for the avoidance or mitigation of secondary events in multiple-event accidents.

7.2 Recommendations for future work

The complexity of addressing this collision mitigation problem in a post-impact scenario is not insignificant. The following issues are considered most critical for improving the design of the proposed post impact control function, especially from the optimal path control point of view:

Seamless interface with driver A number of driver overriding criteria were applied in the driving simulator tests for PIC function verification; these were mostly focused on brake torque superimposition. It is expected that more research can be done to evaluate the human-machine interface between the function and driver requests. For instance, using the EPAS system, an abrupt steering torque input superimposed onto the steering wheel may possibly injure the driver's hands. Hence, it may be necessary to limit the rotational torque applied to the steering wheel, even if this can degrade the controller performance. It is also critical to determine the timing and actions associated with returning control back to the driver, especially to avoid misunderstandings between the vehicle controller and human driver.

Inclusion of the steering actuator may also increase the risk of vehicle motion overshooting after the point of maximum lateral displacement being reached, which may impose a more challenging task for the settling phase. It is expected that in future work, the settling controller should be improved in order to better track a desired profile of vehicle speeds in road coordinates.

Verification in experimental vehicles An important contribution to the further development of PIC function will be to test and validate the control algorithm, especially the actuators' capability, through implementation on experimental vehicles. This is in addition to the aim of verifying driver-machine interaction in a driving simulator; experiments in real vehicles should be able to demonstrate the controller performance either without a driver in the control loop, or with a virtual "post impact driver" model deduced from the studies using driving simulators.

Control arbitration for high CG vehicle For a high CG vehicle, e.g. SUV and light trucks, the roll and lateral acceleration immediately after the initial impact can be so large that path control alone may not be able to mitigate an un-tripped roll-over as the secondary event. Control arbitration needs to be determined in order to best manage the brake and steer requests between PIC function and a separate controller such as Roll Stability Control (RSC) function.

Scenario identification and multi-objective criteria In this thesis, a general form of real-time crash risk and injury cost function was proposed. One particular topic for future research is in the area of further evaluation and parameterization of such a cost function. Depending on the amount of information available about the environment, the *field of safe travel* can be sketched so that a hierarchy of targets for risk reduction can be developed in real-time. For instance, if curved road boundaries are identified from on-line digital maps, path deviation perpendicular to the road boundary at the predicted maximum off-tracking point would be avoided as a priority. Or if collision becomes unavoidable, the priority should switch to crash mitigation so that crash severity is minimized; the optimal strategy depends on the detail and quality of the *scenario identification* and the intended control response should be based on multi-objective criteria.

In the path controller, the displacements were measured at the mass centre, while the paths of the corner points of the vehicle body are especially important for assessing collision consequence. These trajectories can be typically wrapped within an *envelope* which is a curve tangent to each path at some point, and bounds their combined maximum path deviations [103]. This is a relevant issue because the impending secondary collision can happen to any point of the vehicle as a rigid body in the road and off-road map. Therefore, the collision probability can depend on the vehicle yaw angle and also road layout, apart from the trajectory at CG. It is expected that the yaw angle

control can become important as a top-level objective for large path lateral deviation of the mass centre since the vehicle could be exposed to the on-coming traffic.

Sensors and actuators failures It may be that, during the initial impact, some damage is sustained to cause sensors or actuators to fail. Provided faults or partial system failures can be identified in real-time, control adaptation should be feasible. In the case of actuator faults, the constraints on Hamiltonian minimization should take this into account. In other cases, such as sensors for yaw angle estimation being lost, it could be that PIC would default to a simpler control strategy, such as full braking. Similar to the identification of the external scenario, the topic of internal system fault detection, identification and compensation is worthy of much deeper consideration in the future.

References

- [1] U. Sander, K. Mroz, O. Boström, and R. Fredriksson, “The effect of pre-pretensioning in multiple impact crashes,” Autoliv Research, Sweden, Tech. Rep. 09-0333, 2009.
- [2] D. Yang, B. Jacobson, and M. Lidberg, “Benefit prediction of passenger car post impact stability control based on accident statistics and vehicle dynamics simulations,” in *Proc. 21st International Symposium on Dynamics of Vehicles on Roads and Tracks*, Stockholm, Sweden, 2009.
- [3] P. Fay, R. Sferco, and F. Richard, “Multiple Impact Crashes - Consequences for occupant protection measures,” in *Proc. IRCOBI Conference*, Isle of Man, UK, 2001.
- [4] K. Langwieder, A. Sporner, and W. Hell, “RESICO - Retrospective safety analysis of car collisions resulting in serious injuries,” GDV 9810, Munich, Germany, 1999.
- [5] T. Atsushi, M. Daisuke, S. Hidetsugu, P. Chinmoy, and O. Tomosaburo, “An insight into multiple impact crash statistics to search for future directions of counter-approaches,” in *Proc. 22th International Conference on Enhanced Safety of Vehicles (ESV)*, Washington, D.C., 2011.
- [6] U. Sander, “Requirements to occupant restraint systems in multiple impact crashes in-depth analysis of real world accident data,” Master’s Thesis (June 2009), Graz, Austria, Technical University in Graz, public available in 2013.
- [7] J. Zhou, J. Lu, and H. Peng, “Vehicle stabilisation in response to exogenous impulsive disturbances to the vehicle body,” *International Journal of Vehicle Autonomous Systems*, vol. 8, no. Nos. 2/3/4, pp. 242–262, 2010.

REFERENCES

- [8] Robert Bosch GmbH, “10 years of ESP from Bosch - More driving safety with the Electronic Stability Program,” *Corporate Communications*, no. March, 2009. [Online]. Available: www.bosch-presse.de
- [9] A. Van Zanten, *ESP Electronic Stability Program in Robert Bosch GmbH*, 2nd ed. Warrendale, PA: Society of Automotive Engineers, Inc, 1999, pp. 206–243.
- [10] K. Koibuchi, M. Yamaoto, and Y. Fukada, “Vehicle dynamics control in limit cornering by active brake,” *SAE Technical Paper*, no. 960487, 1996.
- [11] M. Naraghi, A. Roshanbin, and A. Tavasoli, “Vehicle stability enhancement - an adaptive optimal approach to the distribution of tyre forces,” *Proc. Institution of Mechanical Engineers, Part D: Journal of Automobile Engineering*, vol. 224, no. 4, pp. 443–453, Apr. 2010.
- [12] K. Yi, T. Chung, J. Kim, and S. Yi, “An investigation into differential braking strategies for vehicle stability control,” *Proc. Institution of Mechanical Engineers, Part D: Journal of Automobile Engineering*, vol. 217, no. 12, pp. 1081–1093, Jan. 2003.
- [13] A. T. Van Zanten, “Evolution of electronic control systems for improving the vehicle dynamic behavior,” in *Proc. 6th International Symposium on Advanced Vehicle Control*, Hiroshima, Japan, 2002.
- [14] A. Linder, T. Dukic, M. Hjort, Y. Matstoms, S. Mårdh, J. Sundström, A. Vadeby, M. Wiklund, and J. Östlund, *Methods for evaluation of traffic safety effects of Antilock Braking System (ABS) and Electronic Stability Control (ESC) - A literature review*. Gothenburg: Swedish National Road and Transport Research Institute (VTI), 2007.
- [15] A. Lie, C. Tingvall, M. Krafft, and A. Kullgren, “The effectiveness of electronic stability control (ESC) in reducing real life crashes and injuries.” *Traffic Injury Prevention*, vol. 7, no. 1, pp. 38–43, 2006.
- [16] S. A. Ferguson, “The effectiveness of electronic stability control in reducing real-world crashes : A literature review,” *Traffic Injury Prevention*, vol. 8, no. 4, pp. 329–338, 2007.
- [17] D. Yang, T. J. Gordon, M. Lidberg, M. Jonasson, and B. Jacobson, “Post-impact vehicle path control by optimization of individual wheel braking sequences,” in *Proc. 10th International Symposium on*

- Advanced Vehicle Control*, Loughborough, United Kingdom, 2010, pp. 882–887.
- [18] J. William Haddon, “The changing approach to the epidemiology, prevention, and amelioration of trauma: the transition to approaches etiologically rather than descriptively based,” *American Journal of Public Health*, vol. 58, no. 8, pp. 1431–1438, 1968.
- [19] Robert Bosch GmbH, “Secondary collision mitigation: Protection against subsequent crashes,” 2010.09.21. [Online]. Available: <http://www.bosch-automotivetechnology.com>
- [20] S. Bickerstaffe, “Conti puts the brakes on secondary collisions - Emergency braking function stops the car after the first impact,” 2012.10.28. [Online]. Available: <http://ae-plus.com/technology/contiputsthebrakesonsecondarycollisions>
- [21] EURO NCAP, “Audi secondary collision brake assist,” 2012.12.05. [Online]. Available: <http://www.euroncap.com/rewards/audisecondarycollisionbrakeassist>
- [22] G. M. Mackay, S. J. Ashton, M. D. Galer, and P. D. Thomas, “The methodology of in-depth studies of car crashes in Britain,” *SAE Technical Paper*, no. 850556, 1985.
- [23] D. Otte, T. Pohlemann, and M. Blauth, “Significance of soft tissue neck injuries AIS 1 in the accident scene and deformation characteristics of cars with delta-V up to 10 km/h,” in *Proc. IRCOBI Conference*, Hannover, Germany, 1997, pp. 265–283.
- [24] D. Otte, C. Haasper, V. Eis, and R. Schaefer, “Characteristics of pole impacts to side of passenger cars in European traffic accidents and assessment of injury mechanisms - Analysis of German and UK in-depth data,” *Stapp Car Crash Journal*, vol. 52, no. November, pp. 349–362, 2008.
- [25] BASt/FAT, “GIDAS (German In-Depth Accident Study) information brochure,” 2009.01.07. [Online]. Available: www.gidas.org
- [26] P. Fay, R. Sferco, and R. Frampton, “Vehicle rollover - An important element in multiple impact crashes,” in *Proc. 18th International Conference on Enhanced Safety of Vehicles (ESV)*, Nagoya, Japan, 2003.

REFERENCES

- [27] J. Bahouth and D. Kennerly, “Characteristics of multiple impact crashes that produce serious injuries,” in *Proc. 19th International Conference on Enhanced Safety of Vehicles (ESV)*, Washington, D.C., USA, 2005.
- [28] T. Miller, J. Viner, S. Rossman, N. Pindus, W. Gellert, J. Douglass, A. Dillingham, and G. Blomquist, “The costs of highway crashes,” USA, 1991.
- [29] J. Zhou, “Active safety measures for vehicles involved in light vehicle-to-vehicle impacts,” Ph.D. dissertation, Mechanical Engineering, University of Michigan, 2009.
- [30] A. Häussler, R. Schäffler, A. Georgi, and S. Stabrey, “Networking of airbag and ESP for prevention of further collisions,” *ATZ - Automobiltechnische Zeitschrift*, vol. 114, pp. 22–26, 2012.
- [31] Y. Shibahata, K. Shimada, and T. Tomari, “Improvement of vehicle maneuverability by direct yaw moment control,” *Vehicle System Dynamics*, vol. 22, no. 5-6, pp. 465–481, 1993.
- [32] M. Blank and D. L. Margolis, “Minimizing the path radius of curvature for collision avoidance minimizing the path radius of curvature for collision avoidance,” *Vehicle System Dynamics*, vol. 33, no. 3, pp. 183–201, 2000.
- [33] J. Edelmann and M. Plöchl, “Handling characteristics and stability of the steady-state powerslide motion of an automobile,” *Regular and Chaotic Dynamics*, vol. 14, no. 6, pp. 682–692, 2009.
- [34] M. Thommyppillai, S. Evangelou, and R. Sharp, “Car driving at the limit by adaptive linear optimal preview control,” *Vehicle System Dynamics*, vol. 47, no. 12, pp. 1531–1550, 2009.
- [35] J. Edelmann, M. Plöchl, and P. Pfeffer, “Analysis of steady-state vehicle handling and driver behaviour at extreme driving conditions,” in *Proc. 22st International Symposium on Dynamics of Vehicles on Roads and Tracks*, Manchester, UK, 2011.
- [36] C. Voser, R. Y. Hindiyeh, and J. C. Gerdes, “Analysis and control of high sideslip manoeuvres,” *Vehicle System Dynamics*, vol. 48, no. sup1, pp. 317–336, 2010.

- [37] E. Velenis, E. Frazzoli, and P. Tsiotras, “Steady-state cornering equilibria and stabilisation for a vehicle during extreme operating conditions,” *International Journal of Vehicle Autonomous Systems*, vol. 8, no. 2/3/4, pp. 217 – 241, 2010.
- [38] K. Kritayakirana and J. C. Gerdes, “Autonomous cornering at the limits: designing a longitudinal feedback controller using a tire slip circle,” in *Proc. 10th International Symposium on Advanced Vehicle Control*, Loughborough, United Kingdom, 2010, pp. 418–423.
- [39] M. Klomp, “Longitudinal force distribution and road vehicle handling,” Ph.D. dissertation, Applied Mechanics, Chalmers University of Technology, 2010.
- [40] C. G. Bobier and J. C. Gerdes, “Staying within the nullcline boundary for vehicle envelope control using a sliding surface,” *Vehicle System Dynamics*, vol. 51, no. 2, pp. 199–217, 2013.
- [41] R. Rajamani, *Vehicle dynamics and control*. Springer, 2006.
- [42] P. Seiler, B. Song, and J. K. Hedrick, “Development of a collision avoidance system,” *SAE Special Publications*, vol. 1332, pp. 97–103, 1998.
- [43] H. Jula, E. B. Kosmatopoulos, and P. A. Ioannou, “Collision avoidance analysis for lane changing and merging,” *IEEE Transactions on Vehicular Technology*, vol. 49, no. 6, pp. 2295–2308, 2000.
- [44] S. K. Gehrig and F. J. Stein, “Collision avoidance for vehicle-following systems,” *IEEE Transactions on Intelligent Transportation Systems*, vol. 8, no. 2, pp. 233–244, 2007.
- [45] J.-L. Su and A. W. Ordys, “Collision avoidance manoeuvre for a vehicle - A practical approach,” *Proc. Institution of Mechanical Engineers, Part D: Journal of Automobile Engineering*, vol. 224, no. 3, pp. 299–312, 2009.
- [46] M. Salfeld, S. Stabrey, and A. Trächtler, “Optimal control inputs to affect vehicle dynamics in various driving states,” in *Proc. 7th IFAC Symposium on Nonlinear Control Systems*, Pretoria, South Africa, 2007.
- [47] M. Salfeld, “Konzeption eines Regelungssystems zur gezielten Beeinflussung der Fahrdynamik in Unfallsituationen,” Ph.D. dissertation, Universität Paderborn Heinz Nixdorf Inst., 2008.

REFERENCES

- [48] S. Stabrey, “Predictive vehicle dynamics control: driver-vehicle-controller interaction,” in *FISITA World Automotive Congress*, Barcelona, Spain, 2004.
- [49] J. Zhou, H. Peng, and J. Lu, “Collision model for vehicle motion prediction after light impacts,” *Vehicle System Dynamics*, vol. 46, no. 1, pp. 3–15, 2008.
- [50] “CarSim information,” 2011.04.16. [Online]. Available: <http://www.carsim.com/products/carsim/index.php>
- [51] E. Pettersson and D. Tidholm, “Vehicle stability control for side collisions by brake and steering wheel torque superposition,” Master’s Thesis 2007:31, ISSN 1652-8557, Gothenburg, Sweden, Chalmers University of Technology, 2007.
- [52] H.-s. Tan and C.-y. Chan, “Design of steering controller and analysis of vehicle lateral dynamics under impulsive disturbances,” in *Proc. American Control Conference*, Chicago, Illinois, 2000, pp. 2023–2027.
- [53] V. L. Neale, T. A. Dingus, S. G. Klauer, J. Sudweeks, and M. Goodman, “An overview of the 100-Car naturalistic study and findings,” USA, p. 5, 2005.
- [54] Vehicle and Traffic Safety Centre at Chalmers (SAFER), “Test Site Sweden Field Operational Test - final report,” Sweden, 2008.
- [55] M. Thor, “The efficiency of electronic stability control after light collisions,” Master’s Thesis 2007:02, ISSN 1652-8557, Gothenburg, Sweden, Chalmers University of Technology, 2007.
- [56] G. Forkenbrock, D. Elsasser, B. O’Harra, and R. Jones, “Development of criteria for electronic stability control performance evaluation,” USA, 2005.
- [57] National Highway and Traffic Safety Administration, “Federal motor vehicle safety standards; Electronic Stability Control systems; controls and displays,” USA, 2008.10.11. [Online]. Available: <https://www.federalregister.gov/articles/2008/09/22/E8-22067>
- [58] G. Markkula, O. Benderius, K. Wolff, and M. Wahde, “A review of near-collision driver behavior models,” *Human Factors: The Journal of the Human Factors and Ergonomics Society*, vol. 54, no. 6, pp. 1117–1143, 2012.

- [59] D. Marco, “What factors influence drivers’ response time for evasive maneuvers in real traffic?” *Accident Analysis and Prevention, in press*, 2012.
- [60] M. Green, “How long does it take to stop?” Methodological analysis of driver perception - brake times,” *Transportation Human Factors*, vol. 2, no. 3, pp. 195–216, 2000.
- [61] A. Kusachov and F. A. Mouatamid, “Post impact braking verification in motion platform simulator,” Master’s Thesis 2012:36, ISSN 1652-8557, Gothenburg, Sweden, Chalmers University of Technology, 2012.
- [62] T. D. Gillespie, *Fundamentals of vehicle dynamics*. Society of Automotive Engineers, Inc, 1992.
- [63] H. B. Pacejka, *Tire and vehicle dynamics*, 2nd ed. Warrendale, PA: Society of Automotive Engineers, Inc, 2006.
- [64] B. Cliff, “Validation of PC-Crash - A momentum-based accident reconstruction program,” *SAE Technical Paper*, no. 960885, 1996.
- [65] S. Hermann and A. Moser, “The collision and trajectory models of PC-Crash,” *SAE Technical Paper*, no. 960886, 1996.
- [66] Raymond M. Brach, *Vehicle accident analysis and reconstruction methods*. Warrendale, PA: SAE International, 2005.
- [67] D. Yang, “Method for benefit prediction of passenger car post impact stability control,” Master’s Thesis 2009:06, ISSN 1652-8557, Gothenburg, Sweden, Chalmers University of Technology, 2009.
- [68] S. Hermann, “Accident reconstruction methods,” *Vehicle System Dynamics*, vol. 47, no. 8, pp. 1049–1073, Aug. 2009.
- [69] BAST/FAT, “The GIDAS Project,” 2011.04.20. [Online]. Available: <http://www.gidas.org/en>
- [70] J. Beltran and Y. Song, “Methods for verification of post impact control including driver interaction,” Master’s Thesis 2011:11, ISSN 1652-8557, Chalmers University of Technology, 2011.
- [71] D. Yang, T. J. Gordon, B. Jacobson, and M. Jonasson, “Quasi-linear optimal path controller applied to post impact vehicle dynamics,” *IEEE Transactions on Intelligent Transportation Systems*, vol. 13, no. 4, pp. 1586–1598, 2012.

REFERENCES

- [72] J. T. Betts, “Survey of numerical methods for trajectory optimization,” *Journal of Guidance Control and Dynamics*, vol. 21, pp. 193–207, 1998.
- [73] I. Ross, *A primer on Pontryagin’s Principle in optimal control*. Collegiate Publishers, 2009.
- [74] J. A. E. Bryson and Y.-C. Ho, *Applied optimal control: Optimization, estimation and control*, revised ed. Taylor & Francis, 1975.
- [75] W. H. Press, S. Teukolsky, W. Vetterling, and B. Flannery, *Numerical recipes: The art of scientific computing*, 3rd ed. Cambridge University Press, 2007.
- [76] J. F. Bonnans, J. C. Gilbert, C. Lemaréchal, and C. A. Sagastizábal, *Numerical optimization - theoretical and practical aspects*, ser. Universitext. Springer Verlag, Berlin, 2006.
- [77] “The MathWorks, documentation, optimization toolbox, functions,” 2009.10.11. [Online]. Available: <http://www.mathworks.com>
- [78] M. Vukov, “Key features of ACADO toolkit,” 2011.06.16. [Online]. Available: <http://sourceforge.net/p/acado/wiki/Features/>
- [79] P. Rutquist and M. M. Edvall, “PROPT - MATLAB optimal control software,” 2012.04.11. [Online]. Available: <http://tomdyn.com/index.html>
- [80] M. A. Patterson and A. V. Rao, “GPOPS - II Version 1.0: A General-Purpose MATLAB toolbox for solving optimal control problems using the Radau Pseudospectral method,” 2013.05.30. [Online]. Available: <http://www.gpops.org/resources/gpops2QuickReference.pdf>
- [81] Modelon AB, “JModelica.org user guide: Version 1.6.0,” 2011.10.28. [Online]. Available: <http://www.jmodelica.org/page/236>
- [82] O. von Stryk, “User’s guide for DIRCOL (version 2.1): A direct collocation method for the numerical solution of optimal control problems,” *Fachgebiet Simulation und Systemoptimierung (SIM)*, 1999.
- [83] A. Wächter and L. T. Biegler, “On the implementation of an interior-point filter line-search algorithm for large-scale nonlinear programming,” *Mathematical Programming*, vol. 106, no. 1, pp. 25–57, 2006. [Online]. Available: <http://dx.doi.org/10.1007/s10107-004-0559-y>

- [84] P. E. Gill and W. M. Murray and M. A. Saunders, “User’s manual for SNOPT Version 7: Software for large-scale nonlinear programming,” 2013.05.30. [Online]. Available: <http://www.ccom.ucsd.edu/~peg/papers/sndoc7.pdf>
- [85] J. Åkesson, K.-E. Årzén, M. Gäfvert, T. Bergdahl, and H. Tummescheit, “Modeling and optimization with Optimica and JModelica.org - Languages and tools for solving large-scale dynamic optimization problem,” *Computers and Chemical Engineering*, vol. 34, no. 11, pp. 1737–1749, 2010.
- [86] H. K. Khalil, *Nonlinear Systems*, 3rd ed. New Jersey: Prentice Hall, Inc., 2002.
- [87] B.-j. Kim and H. Peng, “Vehicle stability control of heading angle and lateral deviation to mitigate secondary collisions,” in *Proc. 11th International Symposium on Advanced Vehicle Control*, Seoul, Korea, 2012.
- [88] M. Jonasson, J. Andreasson, B. Jacobson, and A. S. Trigell, “Global force potential of over-actuated vehicles,” *Vehicle System Dynamics*, vol. 48, no. 9, pp. 983–998, 2010.
- [89] J. J. Gibson and L. E. Crooks, “A theoretical field-analysis of automobile-driving,” *The American Journal of Psychology*, vol. 51, no. 3, pp. 453–471, 1938.
- [90] P. Falcone, E. H. Tseng, F. Borrelli, J. Asgari, and D. Hrovat, “MPC-based yaw and lateral stabilisation via active front steering and braking,” *Vehicle System Dynamics*, vol. 46, no. sup1, pp. 611–628, 2008.
- [91] H. Yoshida, S. Shinohara, and M. Nagai, “Lane change steering manoeuvre using model predictive control theory,” *Vehicle System Dynamics*, vol. 46, no. sup1, pp. 669–681, 2008.
- [92] J. Edelmann, M. Plöchl, W. Reinalter, and W. Tieber, “A passenger car driver model for higher lateral accelerations,” *Vehicle System Dynamics*, vol. 45, no. 12, pp. 1117–1129, 2007.
- [93] B. D. O. Anderson and J. B. Moore, *Optimal control: Linear Quadratic methods*. Upper Saddle River, NJ, USA: Prentice-Hall, Inc., 1990.
- [94] D. Yang, M. Jonasson, B. Jacobson, and T. J. Gordon, “Closed-loop controller for post-impact vehicle dynamics using individual wheel

REFERENCES

- braking and front axle steering,” *submitted for publication in International Journal of Vehicle Autonomous Systems*, 2013.
- [95] D. Q. Mayne, J. B. Rawlings, C. V. Rao, and P. O. M. Scokaert, “Constrained model predictive control: Stability and optimality,” *Automatica*, vol. 36, 2000.
- [96] M. Morari and J. H. Lee, “Model predictive control: Past, present and future,” *Computers and Chemical Engineering*, vol. 23, 1999.
- [97] B. Pluymers, L. Roobrouck, J. Buijs, J. A. K. Suykens, and B. De Moor, “Constrained linear MPC with time-varying terminal cost using convex combinations,” *Automatica*, vol. 41, no. 5, pp. 831–837, 2005.
- [98] W. Chen, D. J. Ballance, and J. O’Reilly, “Model predictive control of nonlinear systems: Computational burden and stability,” *IEEE Proc.: Control Theory and Applications*, vol. 147, no. 4, pp. 387–392, 2000.
- [99] “PIT maneuver,” 2011.04.25. [Online]. Available: http://en.wikipedia.org/wiki/PIT_maneuver
- [100] “Wet grip area, kick plate,” 2011.04.27. [Online]. Available: <http://development.rockingham.co.uk/oem/wetgrip.asp>
- [101] “Skid plates for cars, trucks, and motorcycles,” 2011.04.27. [Online]. Available: <http://www.hmp-bau.com/Product.29.0.html?&L=2>
- [102] “Driving Simulator IV in VTI,” 2013.04.27. [Online]. Available: <http://www.vti.se/sv/forskningsomraden/fordonsteknik/vtis-simulatorer>
- [103] “Envelop (mathematics),” 2010.10.11. [Online]. Available: <http://en.wikipedia.org/wiki/Envelope>

Nomenclature and Glossary

Roman symbols

F_{wi}	[N]	Brake pad force on wheel i
F_{xwi}	[N]	Requested brake force, transformed from brake pad force to tyre i
F_{xi}	[N]	Longitudinal force on wheel i , in vehicle coordinate
F_{xg}	[N]	Aggregated longitudinal force on body, in road coordinate
F_{yi}	[N]	Lateral force on wheel i , in vehicle coordinate
F_{yg}	[N]	Aggregated lateral force on body, in road coordinate
F_{zi}	[N]	Vertical force on wheel i , in vehicle coordinate
F_{zg}	[N]	Aggregated vertical force on body, in road coordinate
H	[-]	Hamiltonian, a scalar function to be minimized
I_{xx}	[kg m ²]	Roll moment of inertia
I_{yy}	[kg m ²]	Pitch moment of inertia
I_{zz}	[kg m ²]	Yaw moment of inertia
J	[-]	Cost functional of an optimization problem
X	[m]	Vehicle longitudinal displacement, in road coordinate
Y	[m]	Vehicle lateral displacement, in road coordinate
Z	[m]	Vehicle vertical displacement, in road coordinate
g	[m/s ²]	Gravitational acceleration
m	[kg]	Vehicle mass
v	[m/s]	Vehicle speed: $\sqrt{v_x^2 + v_y^2}$
v_x	[m/s]	Longitudinal velocity, in vehicle coordinate
v_y	[m/s]	Lateral velocity, in vehicle coordinate

Greek symbols

Δv	[km/h]	Speed change during an impact
α_i	[rad]	Tyre side slip angle
β	[rad]	Vehicle side slip angle: $\arctan(v_y/ v_x)$
δ_f	[rad]	Road wheel steer angle at front axle
ψ	[rad]	Vehicle yaw angle
$\dot{\psi}$	[rad]	Vehicle yaw rate
ϕ	[rad]	Vehicle roll angle
$\dot{\phi}$	[rad]	Vehicle roll rate
θ	[rad]	Vehicle pitch angle
$\dot{\theta}$	[rad]	Vehicle pitch rate
μ	[-]	Road friction coefficient
λ	[-]	Lagrange multiplier vector whose elements are called <i>co-states</i>

Subscripts and superscripts

<i>act</i>	<i>active</i> contributions from brake torques and steer angle inputs
f	final, final time defined in optimal control problem
<i>g</i>	quantities expressed in <i>global</i> road coordinates
<i>i</i>	1: front left tyre, 2: front right tyre, 3: rear left tyre, 4: rear right tyre
PI	Post-Impact, instant immediate after initial impact
*	<i>optimal</i> control quantities

Abbreviations

ABS	Anti-lock Brake System
ABL	Active Bending Lights
ACC	Adaptive Cruise Control
ADAS	Advanced Driver Assistance System
AEB	Autonomous Emergency Braking
AIS	Abbreviated Injury Scale
ASR	Anti-Slip Regulation
BLIS	Blind Spot Info System
BVP	Boundary Value Problem
CG	Centre of Gravity
DAC	Driver Alert Control
DAEs	Differential Algebraic Equations
DOF	Degree of Freedom
ECU	Electronic Control Unit
ESC	Electronic Stability Control
EPAS	Electric Power Assist Steering
FOTs	Field Operational Tests
GIDAS	Germany In-depth Accident Study
GPS	Global Positioning System
IC	Inflatable Curtain
IDIS	Intelligent Driver Information System
LDW	Lane Departure Warning
LKAS	Lane Keep Assist System
LQ	Linear Quadratic
MEAs	Multiple-Event Accidents
NLP	Nonlinear Programming
NMPC	Nonlinear Model Predictive Control
ODEs	Ordinary Differential Equations
PIB	Post Impact Braking
PIC	Post Impact Control
PISC	Post Impact Stability Control
RSC	Roll Stability Control
RWS	Rear Wheel Steering
SEAs	Single-Event Accidents
SCM	Secondary Collision Mitigation
SUV	Sport Utility Vehicle
TPMS	Tire Pressure Monitoring System
WHIPS	Whiplash Protection System

